

Experiments to Test

Flash chambers discharging like neon lights, giant spectrometers, stacks of crystals, tons of plastic scintillators, thousands of precisely strung wires—all employed to test the ideas of unified field theories.

It has long been a dream of physicists to produce a unified field theory of the forces in nature. Much of the current experimental work designed to test such theories occurs at the highest energies capable of being produced by the latest accelerators. However, elegant experiments can be designed at lower energies that probe the details of the electroweak theory (in which the electromagnetic and weak interactions have been partially unified) and address key questions about the further unification of the electroweak and the strong interactions. (See “An Experimentalist’s View of the Standard Model” for a brief look at the current status of the quest for a unified field theory.)

In this article we will describe four such experiments being conducted at Los Alamos, often with outside collaborators. The first, a careful study of the beta decay of tritium, is an attempt to determine whether or not the neutrino has a mass and thus whether or not there can be mixing between the three known lepton families (the electron, muon, and tau and their associated neutrinos).

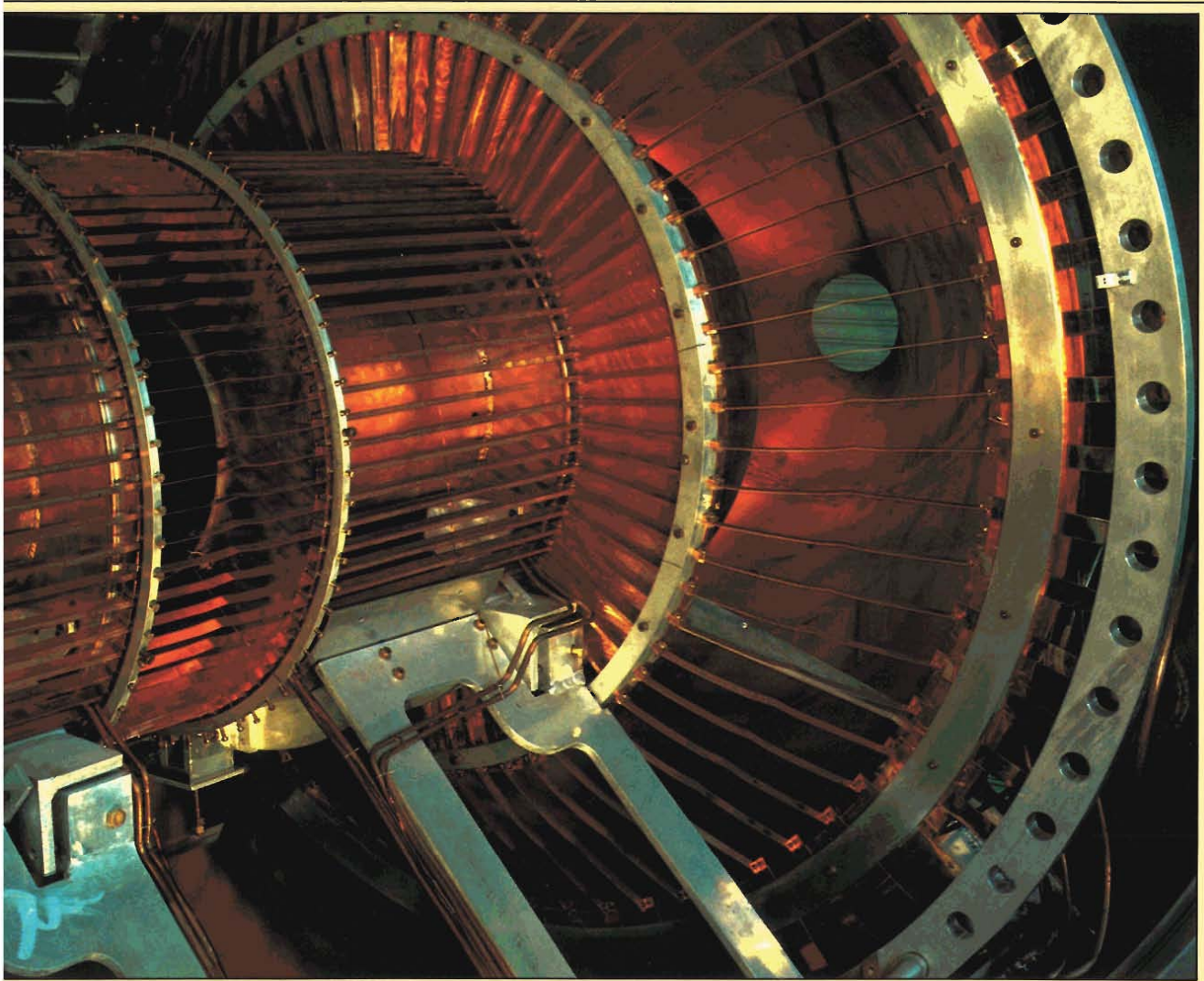
Two other experiments examine the decay of the muon. The first is a search for *rare* decays that do not involve neutrinos, that is, the direct conversion across lepton families of the muon to an electron. The muon is a duplicate, except for a greater mass, of the electron, making such a decay seem almost mandatory. Detection of a rare decay, or even the lowering of the limits for its occurrence, would tell us once again more about the mixing between lepton families and about possible violation of lepton conservation laws. At the same time, precision studies of ordinary muon decay, in which neutrinos are generated (the muon is accompanied by its own neutrino and thereby preserves muon number), will help test the structure of the present theory describing the weak interaction, for example, by setting limits on whether or not parity conservation is restored as a symmetry at high energies.

The electron spectrometer for the tritium beta decay experiment under construction. The thin copper strips evident in the entrance cone region to the right and at the first narrow region toward the center are responsible for the greatly improved transmission of this spectrometer.



Unification Schemes

by Gary H. Sanders



John Flower

The intent of the fourth experiment is to measure interference effects between the neutral and charged weak currents via scattering experiments with neutrinos and electrons. If destructive interference is detected, then the present electroweak theory should be applicable even at higher energies; if constructive interference is detected, then the theory will need to be expanded, say by including vector bosons beyond those (the Z^0 and the W^\pm) already in the standard model.

Tritium Beta Decay

In 1930 Pauli argued that the continuous kinetic energy spectrum of electrons emitted in beta decay would be explained by a light, neutral particle. This particle, the neutrino, was used by Fermi in 1934 to account quantitatively for the kinematics of beta decay. In 1953, the elusive neutrino was observed directly by a Los Alamos team, Fred Reines and Clyde L. Cowan, using a reactor at Hanford.

Though the neutrino has generally been taken to be massless, no theory requires neutrinos to have zero mass. The current experimental upper limit on the electron neutrino mass is 55 electron volts (eV), and the Russian team responsible for this limit claims a lower limit of 20 eV. The mass of the neutrino is still generally taken to be zero, for historical reasons, because the experiments done by the Russian team are extremely complex, and because masslessness leads to a pleasing simplification of the theory.

A more careful look, however, shows that no respectable theory requires a mass that is identically zero. Since we have many neutrino flavors (electron, muon and tau neutrinos, at least), a nonzero mass would immediately open possibilities for mixing between these three known lepton families. Without regard to the minimal standard model or any unification schemes, the possible existence of massive neutrinos points out our basic ignorance of the origin of the known particle masses and the family structure of particles.

An Experimentalist's View of the Standard Model

The dream of physicists to produce a unified field theory has, at different times in the history of physics, appeared in a different light. For example, one of the most astounding intellectual achievements in nineteenth century physics was the realization that electric forces and magnetic forces (and their corresponding fields) are different manifestations of a single electromagnetic field. Maxwell's construction of the differential equations relating these two fields paved the way for their later relation to special relativity.

QED. The most successful field theory to date, quantum electrodynamics (QED), appears to have provided us with a complete description of the electromagnetic force. This theory has withstood an extraordinary array of precision tests in atomic, nuclear, and particle physics, and at low and high energies. A generation of physicists has yearned for comparable field theories describing the remaining forces: the weak interaction, the strong interaction, and gravity.

An even more romantic goal has been the notion that a *single* field theory might describe all the known physical interactions.

Electroweak Theory. In the last two decades we have come a long way towards realizing this goal. The electromagnetic and weak interactions appear to be well described by the Weinberg-Salam-Glashow model that unifies the two fields in a gauge theory. (See "Particle Physics and the Standard Model" for a discussion of gauge theories and other details just briefly mentioned here.) This

electroweak theory appears to account for the apparent difference, at low energies, between the weak interaction and the electromagnetic interaction. As the energy of an interaction increases, a unification is achieved.

So far, at energies accessible to modern high-energy accelerators, the theory is supported by experiment. In fact, the discovery at CERN in 1983 of the heavy vector bosons W^+ , W^- , and Z^0 , whose large mass (compared to the photon) accounts for the relatively "weak" nature of the weak force, beautifully confirms and reinforces the new theory.

The electroweak theory has many experimental triumphs, but experimental physicists have been encouraged to press ever harder to test the theory, to explore its range of validity, and to search for new fundamental interactions and particles. The experience with QED, which has survived decades of precision tests, is the standard by which to judge tests of the newest field theories.

QCD. A recent, successful field theory that describes the strong force is quantum chromodynamics (QCD). In this theory the strong force is mediated by the exchange of color gluons and a coupling constant is determined analogous to the fine structure constant of the electroweak theory.

Standard Model. QCD and the electroweak theory are now embedded and united in the minimal standard model. This model organizes all three fields in a gauge

Table**The first three generations of elementary particles.**

Family:	I	II	III
Doublers {			
Quarks:	$\begin{pmatrix} u \\ d \end{pmatrix}_L$	$\begin{pmatrix} c \\ s \end{pmatrix}_L$	$\begin{pmatrix} t \\ b \end{pmatrix}_L$
Leptons:	$\begin{pmatrix} \nu_e \\ e \end{pmatrix}_L$	$\begin{pmatrix} \nu_\mu \\ \mu \end{pmatrix}_L$	$\begin{pmatrix} \nu_\tau \\ \tau \end{pmatrix}_L$
Singlets:	$u_R, d_R, e_R,$	$c_R, s_R, \mu_R,$	t_R, b_R, τ_R

theory of electroweak and strong interactions. There are two classes of particles: spin- $\frac{1}{2}$ particles called fermions (quarks and leptons) that make up the particles of ordinary matter, and spin-1 particles called bosons that account for the interactions between the fermions.

In this theory the fermions are grouped asymmetrically according to the "handedness" of their spin to account for the experimentally observed violation of CP symmetry. Particles with right-handed spin are grouped in pairs or doublets; particles with left-handed spin are placed in singlets. The exchange of a charged vector boson can convert one particle in a given doublet to the other, whereas the singlet particles have no weak charge and so do not undergo such transitions.

The Table shows how the model, using this scheme, builds the first three generations of leptons and quarks. Since each quark (u , d , c , s , t , and b) comes in three colors and all fermions have antiparticles, the model includes 90 fundamental fermions.

The spin-1 boson mediating the electromagnetic force is a massless gauge boson,

that is, the photon γ . For the weak force, there are both neutral and charged currents that involve, respectively, the exchange of the neutral vector boson Z^0 and the charged vector bosons W^+ and W^- . The color force of QCD involves eight bosons called gluons that carry the color charge.

The coupling constants for the weak and electromagnetic interactions, g_{wk} and g_{em} , are related by the Weinberg angle θ_w , a mixing angle used in the theory to parametrize the combination of the weak and electromagnetic gauge fields. Specifically,

$$\sin \theta_w = g_{em}/g_{wk}.$$

Only objects required by experimental results are in the standard model, hence the term minimal. For example, no right-handed neutrinos are included. Other minimal assumptions are massless neutrinos and no requirement for conservation of total lepton number or of individual lepton flavor (that is, electron, muon, or tau number).

The theory, in fact, includes no mass for any of the elementary particles. Since the

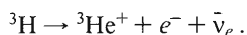
vector bosons for the weak force and all the fermions (except perhaps the neutrinos) are known to be massive, the symmetry of the theory has to be broken. Such symmetry-breaking is accomplished by the Higgs mechanism in which another gauge field with its yet unseen Higgs particle is built into the theory. However, no other Higgs-type particles are included.

Many important features are built into the minimal standard model. For example, low-energy, charged-current weak interactions are dominated by $V-A$ (vector minus axial vector) currents; thus, only left-handed W^\pm bosons have been included. Also, since neutrinos are taken to be massless, there are supposed to be no oscillations between neutrino flavors.

There are many possibilities for extensions to the standard model. New bosons, families of particles, or fundamental interactions may be discovered, or new substructures or symmetries may be required. The standard model, at this moment, has no demonstrated flaws, but there are many potential sources of trouble (or enlightenment).

GUT. One of the most dramatic notions that goes beyond the standard model is the grand unified theory (GUT). In such a theory, the coupling constants in the electroweak and strong sectors run together at extremely high energies (10^{15} to 10^{19} gigaelectron volts (GeV)). All the fields are unified under a single group structure, and a new object, the X , appears to generate this grand symmetry group. This very high-energy mass scale is not directly accessible at any conceivable accelerator. To explore the wilderness between present mass scales and the GUT scale, alas, all high-energy physicists will have to be content to work as low-energy physicists. Some seers believe the wilderness will be a desert, devoid of striking new physics. In the likely event that the desert is found blooming with unexplored phenomena, the journey through this terra incognita will be a long and fruitful one, even if we are restricted to feasible tools. ■

The reaction studied by all of the experiments mentioned is



This simple decay produces a spectrum of electrons with a definite *end point energy* (that is, conservation of energy in the reaction does not allow electrons to be emitted with energies higher than the end point energy). In the absence of neutrino mass, the spectrum, including this end point energy, can be calculated with considerable precision. Any experiment searching for a nonzero mass must measure the spectrum with sufficient resolution and control of systematic effects to determine if there is a deviation from the expected behavior.

Specifically, an end point energy lower than expected would be indicative of energy carried away as mass by the neutrino.

In 1972 Karl-Erik Bergkvist of the University of Stockholm reported that the mass of the electron antineutrino $\bar{\nu}_e$ was less than 55 eV. This experiment used tritium embedded in an aluminum oxide base and had a resolution of 50 eV. The Russian team set out to improve upon this result using a better spectrometer and tritium bound in valine molecules.

Valine is an organic compound, an amino acid. A molecular biologist in the Russian collaboration provided the expertise necessary to tag several of the hydrogen sites on the molecule with tritium. This knowledge is important since one of the effects limiting the accuracy of the result is the knowledge of the final molecular states after the decay.

Also important was the accurate determination of the *spectrometer resolution function*, which involved a measurement of the energy loss of the beta electrons in the valine. This was accomplished by placing an ytterbium-169 beta source in an identical source assembly and measuring the energy loss of these electrons as they passed through the valine.

The beta particles emitted from the source were analyzed magnetically in a toroidal beta

spectrometer. This kind of spectrometer provides the largest acceptance for a given resolution of any known design, and the Russians made very significant advances. The Los Alamos research group, as we shall see, has improved the spectrometer design even further.

In 1980 the Russian group published a positive result for the electron antineutrino mass. After including corrections for the uncertainties in resolution and the final state spectrum, they quoted a 99 per cent confidence level value of

$$14 < m_{\bar{\nu}_e} < 46 \text{ eV}.$$

The result was received with great excitement, but two specific criticisms emerged. John J. Simpson of the University of Guelph pointed out that the spectrometer resolution was estimated neglecting the intrinsic linewidth of the spectrum of the ytterbium-169 calibration source. The experimenters then measured the source linewidth to be 6.3 eV; their revised analysis lowered the best value of the neutrino mass from 34.3 to 28 eV. The basic result of a finite mass survives this reanalysis, according to the authors, but it should be noted that the result is very sensitive to the calibration linewidth. Felix Boehm of the California Institute of Technology has observed that with an intrinsic linewidth of only 9 eV, the 99 per cent confidence level result would become consistent with zero.

The second criticism related to the assumption made about the energy of the final atomic states of helium-3. The valine molecule provides a complex environment, and the branching ratios into the 2s and 1s states of helium-3 are difficult to estimate. Thus the published result may prove to be false.

This discussion illustrates the difficulty of experiments of this kind. Each effort produces, in addition to the published measurement, a roadmap to the next generation experiment. The Russian team built upon its 1980 result and produced a substantially improved apparatus that yielded a new meas-

urement in 1983.

The spectrometer was improved by adding an electrostatic field between the source and the magnetic spectrometer that could be used to accelerate the incoming electrons. The beta spectrum could then be measured, under conditions of constant magnetic field, by sweeping the electrostatic field to select different portions of the spectrum. This technique (originally suggested by the Los Alamos group) provides a number of advantages. The magnetic spectrometer always sees electrons in the same energy range, providing constant detection efficiency throughout the measured spectrum. The magnetic field can also be set above the beta spectrum end point with the electrostatic field accelerating electrons from decays in the source into the spectrometer acceptance. This reduces the background by a large factor by making the spectrometer insensitive to electrons from decays of tritium contamination in the spectrometer volume.

Also, finite source size, which produces a larger image at the spectrometer focal plane, was optically reduced by improved focusing at the source, yielding a higher count rate with better resolution.

The improved spectrometer had a resolution of 25 eV, compared to 45 eV in the 1980 experiment. Background was reduced by a factor of 20, and the region of the spectrum scanned was increased from 700 eV to 1750 eV.

The controversial spectrometer resolution function was determined using a different line of the ytterbium-169 source, and the Russians measured its intrinsic linewidth to be 14.7 eV. They also studied ionization losses by measuring the ytterbium-169 spectrum through varying thicknesses of valine, yielding a considerably more accurate resolution function.

The data were taken in 35 separate runs and the beta spectrum (Fig. 1) was fit by an expression that included the ideal spectral shape and the experimental corrections. The best fit gave

$$m_{\bar{\nu}_e} = 33.0 \pm 1.1 \text{ eV},$$

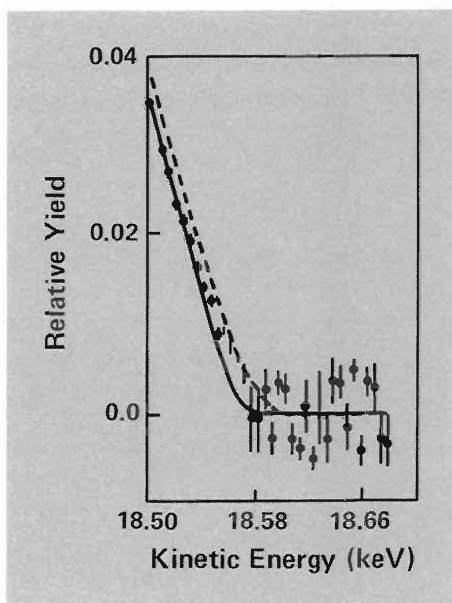


Fig. 1. Electron energy spectrum for tritium decay. This figure shows the 1983 Russian data as the spectrum drops toward an end point energy of about 18.58 keV. The difference in the best fit to the data (solid line) and the fit for a zero neutrino mass (dashed line) is a shift to lower energies that corresponds to a mass of about 33.0 eV. (Figure adapted from Michael H. Shaevitz, "Experimental Results on Neutrino Masses and Neutrino Oscillations," page 140, in *Proceedings of the 1983 International Symposium on Lepton and Photon Interactions at High Energies*, edited by David G. Cassel and David L. Kreinick (Ithaca, New York: F.R. Newman Laboratory of Nuclear Studies, Cornell University, 1983).)

with a 99 per cent confidence limit range of

$$20 < m_{\bar{\nu}_e} < 55 \text{ eV}.$$

These results were derived by making particular choices for the final state spectra. Different assumptions for the valine molecu-

lar final states and the helium-3 molecular, atomic, and nuclear final states can produce widely varying results.

The physics community has been tantalized by the prospect that neutrinos have significant masses. Lepton flavor transitions, neutrino oscillations, and many other phenomena would be expected if the result is confirmed. The range of systematic effects, however, urges caution and enhanced efforts by experimenters to attack this problem in an independent manner. There are currently more than a dozen groups around the world engaged in improved experiments on tritium beta decay. A wide range of tritium sources, beta spectrometers, and analysis techniques are being employed.

The Tritium Source. In an ambitious attempt to use the simplest possible tritium source, a team from a broad array of technical fields at Los Alamos is attempting to develop a source that consists of a gas of free (unbound) tritium atoms. Combining diverse capabilities in experimental particle physics, nuclear physics, spectrometer design, cryogenics, tritium handling, ultraviolet laser technology, and materials science, this team has developed a nearly ideal source and has made numerous improvements in electrostatic-magnetic beta spectrometers.

The two most significant problems come from the scattering and energy loss of the electrons in the source and from the atomic and molecular final states of the helium-3 daughter. These effects are associated with any solid source. Thus the ideal source would appear to be free tritium nuclei, but this is ruled impractical by the repulsive effects of their charge.

The next best source is a gas of free tritium atoms. Detailed and accurate calculations of the atomic final states and electron energy losses can be performed. Molecular effects, including final state interactions, breakup, and energy loss in the substrate, are eliminated. Since the gas contains no inert atoms, the effect of energy loss and scattering in the source are reduced accordingly. Even the measurement of the beta spectrometer

resolution function is simplified.

The forbidding technical problem of such a design is building a source rich enough and compact enough to yield a useful count rate. Only one decay in 10^7 produces an electron with energy in the interesting region near the end point where the spectrum is sensitive to neutrino mass.

The Los Alamos group was motivated by a 1979 talk given by Gerard Stephenson, of the Physics and Theoretical Divisions, on neutrino masses. They recognized quite early, in fact before the 1980 Russian result, that atomic tritium would be a nearly ideal source. In their first design, molecular tritium was to be passed through an extensive gas handling and purification system and atomic tritium prepared using a discharge in a radio-frequency dissociator. The pure jet of atomic tritium was then to be monitored for beta decays. It was clear, however, that the tritium atoms needed to be used more efficiently.

Key suggestions were made at this point by John Browne of the Physics Division and Daniel Kleppner of the Massachusetts Institute of Technology. Advances had been made in the production of dense gases of spin-polarized hydrogen. The new techniques—in which the atomic beam was cooled and then contained in a bottle made of carefully chosen materials observed to have a low probability for promoting recombination of the atoms—promised a possible intense source of free atomic tritium. The collaboration set out to develop and demonstrate this idea. Crucial to the effort was the participation of Laboratory cryogenics specialists.

The resulting tritium source (Fig. 2) circulates molecular tritium through a radio-frequency dissociator into a special tube of aluminum and aluminum oxide. Because the recombination rate for this material near 120 kelvins is very low, the system achieves 80 to 90 per cent purity of atomic tritium. The electrons from the beta decay of the atomic tritium are captured by a magnetic field, and then electrostatic acceleration, similar to that employed by the Russians, is used to trans-

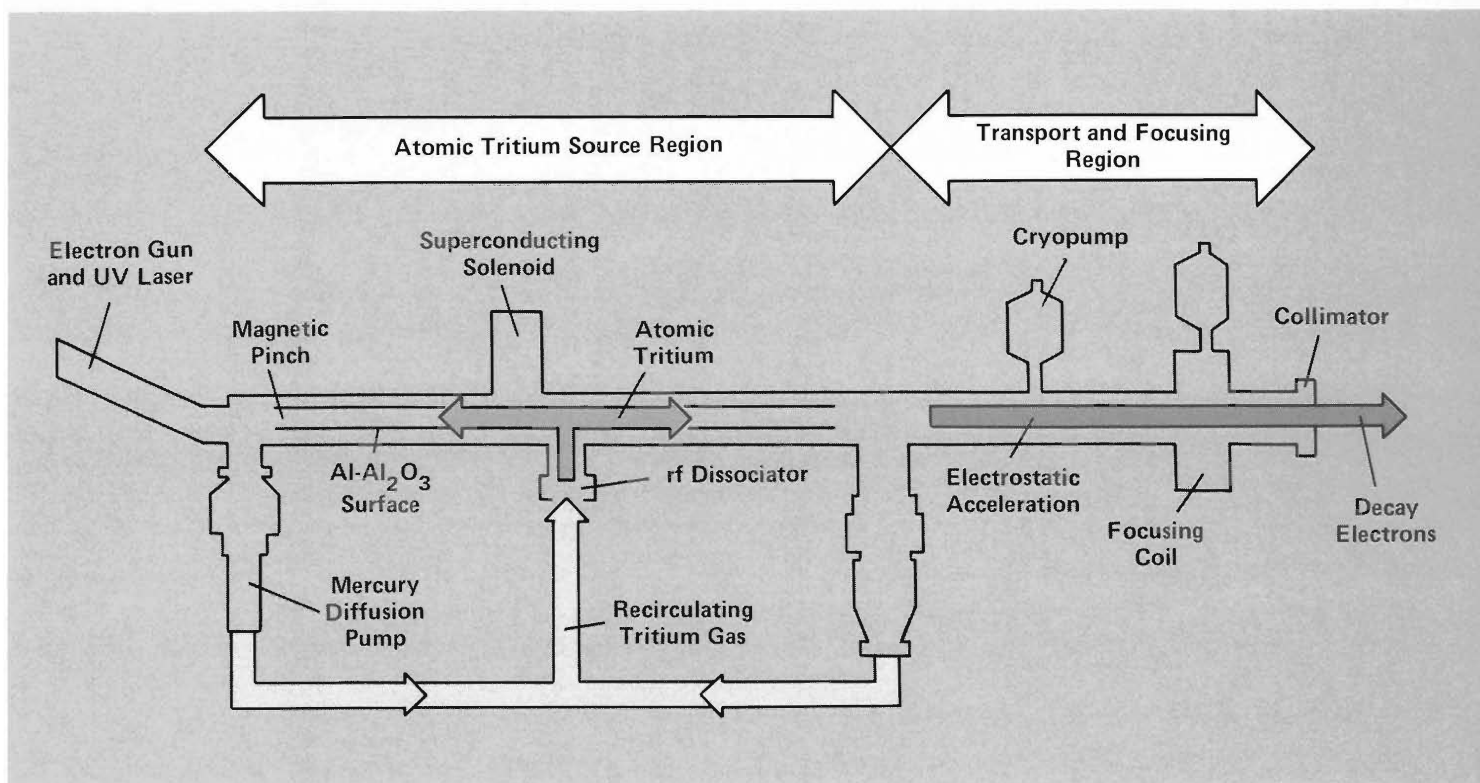


Fig. 2. The tritium source. Molecular tritium passes through the radio-frequency dissociator and then into a 4-meter-long tube as a gas of free atoms. The tube—aluminum with a surface layer of aluminum oxide—has a narrow range around a temperature of 120 kelvins at which the molecular recombination rate is very low, permitting an atom to experience approximately 50,000 collisions before a molecule is formed. The resulting diffuse atomic gas fills the tube, and mercury-diffusion pumps at the ends recirculate it through the dissociator. Typically, the system achieves 80 to 90 per cent purity of atomic tritium. By measuring the spectrum when the dissociator is off, the contribution from the 10 to 20 per cent contamination of molecular tritium can

be determined and subtracted, resulting in a pure atomic tritium electron spectrum.

A superconducting coil surrounds the tube with a field of 1.5 kilogauss. At one end the winding has a reflecting field provided by a magnetic pinch. These fields capture electrons from beta decays with 95 per cent efficiency.

The other end of the tube connects to a vacuum region and has coils that transport and, importantly, focus an image of the electrons into the spectrometer (Fig 3). The tube is held at a selected voltage between -4 and -20 kilovolts, and electrons exit the source to ground potential. Thus, electrons from decays in the source tube are accelerated by a known amount to an energy above that of electrons from decays in

port the electrons toward the spectrometer. During this transport, focusing coils and a collimator are used to form a small image of the electron source in the spectrometer.

Development of this tritium source required solving an array of problems associated with a system that was to recirculate atomic tritium. Everything had to be extremely clean, and no organic materials were allowed; all surfaces are glass or metal. Conducting materials had to be used wherever insulators could collect charge and introduce a bias. The aluminum oxide coating in the tube is so thin that electrons simply tunnel through it, thus providing a conducting surface that does not encourage recombination. Special mercury-diffusion pumps and custom cryopumps, free of oil or other organic materials, had to be fabricated. Every part of the tritium source was an exercise in materials science.

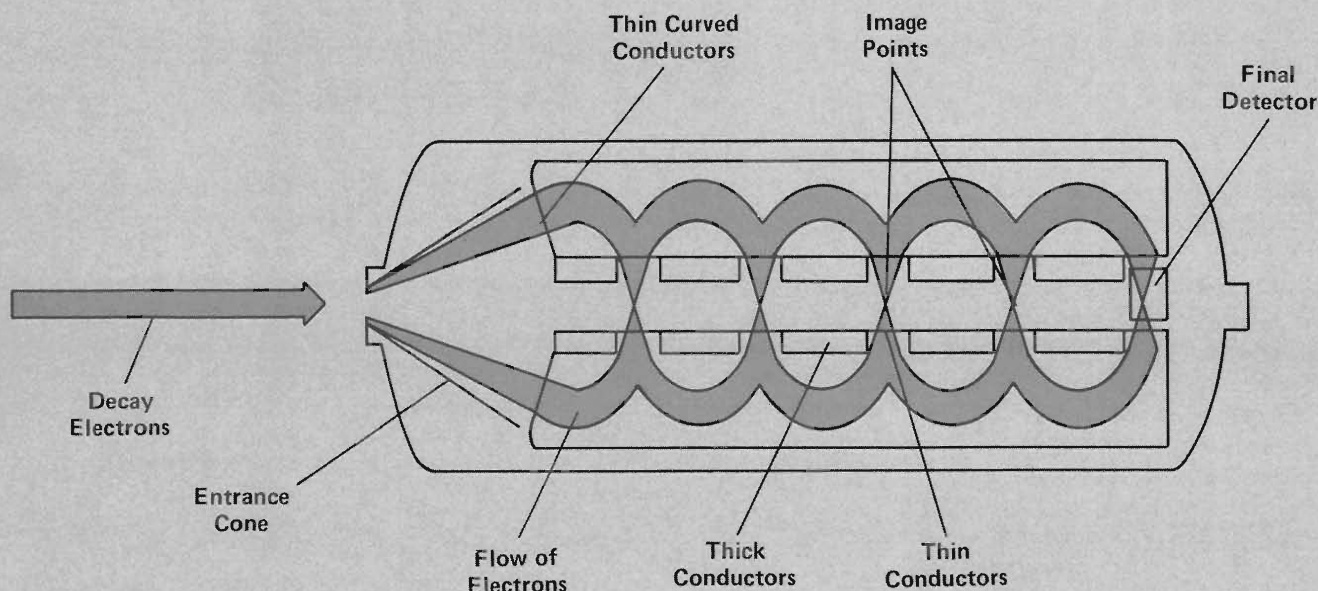
The idea of using electrostatic acceleration at the output of the source was first proposed by the group at Los Alamos in 1980 and subsequently used in the measurement described in the 1983 Russian publication. Accelerating the electrons to an energy above that of electrons from tritium that decays in the spectrometer both strongly reduces the background and also improves the acceptance of electrons into the spectrometer. However, this technique necessitates a larger spectrometer.

There are two other important systematic effects that need to be dealt with: the source image seen by the spectrometer should be small, and electrons produced by decays in the tube that suffer scattering off the walls have an energy loss that distorts the measured spectrum. The focusing coil and the final collimator address both effects, providing a small image. The only energy

loss mechanism remaining is in the tritium gas itself, where losses are less than 2 eV.

The Spectrometer. In addition to cryogenics, tritium handling, and laser technology, the Laboratory's powerful computing capabilities were employed in both the detailed optical design of the beta-electron spectrometer and in extensive Monte-Carlo modeling.

The spectrometer (Fig. 3) is an ambitious development of the Russian design. Electrons from the source pass through the entrance cone and are focused onto the spectrometer axis. One very significant improvement in the spectrometer is the design of the conductors running parallel to the spectrometer axis that do this focusing. In the Russian apparatus, the conductors were thick water-cooled tubes. Most electrons strike the tubes and, as a result of this loss,



the spectrometer. Additional pumps also sharply reduce the amount of tritium escaping into the spectrometer.

Several sophisticated diagnostic systems monitor source output and stability. Beta detectors mounted in the focus region in front of the collimator measure the total decay rate from molecular and atomic tritium, whereas the fraction of tritium in molecular form is monitored by an ultraviolet (1027 angstroms wavelength) laser system developed by members of Chemistry Division that uses absorption lines of molecular tritium. A high-resolution electron gun is used to monitor energy loss in both the gas and the spectrometer. This gun is also used to measure the important spectrometer resolution function directly.

Fig. 3. The spectrometer. Electrons from the source (Fig. 2) that pass through the collimator (with an approximate aperture of 1 centimeter) open into a cone shaped region in the spectrometer with a maximum half angle of 30 degrees. Electrons between 20 and 30 degrees pass between thin conducting strips into the spectrometer and are focused onto the spectrometer axis. This focus serves as a virtual image of the source. Transmission has been greatly improved over the Russian design through the use of thin conductors in all regions of electron flow (see opening photograph for a view of these conductors). The final focal plane detector is a position-sensitive, multi-wire proportional gas counter, also an improvement over previous detectors.

their spectrometer has low transmission.

The Los Alamos spectrometer uses thin 20-mil strips for each of the conductors in the region within the transport aperture. This achieves an order of magnitude higher transmission, essential in yielding a useful count rate in an experiment with a dilute gas source.

Another benefit of the thin strips is that they can be formed easily. In fact, optical calculations accurate to third order dictate the curvature of the entrance and exit strips. The improved focusing properties of this arrangement yield an acceptance three times higher than the Russian device with no compromise in resolution.

The experimenters expect to be taking data throughout the latter part of 1984. They expect an order of magnitude less background and an order of magnitude larger geometric acceptance than the Russian ex-

periment. The design calls for a resolution between 20 and 30 eV, with a sensitivity to neutrino masses less than 10 eV. Even with their dilute gas source, they estimate a data rate in the region within 100 eV of the spectrum end point of about 1 hertz, fully competitive with rates obtained using solid sources.

Many groups around the world are vigorously pursuing this measurement. No other effort, however, will produce a result as free of systematic problems as the Los Alamos project. Other experiments are employing solid sources or, at best, molecular sources. Many have adopted an electrostatic grid system that introduces its own problems. To date, no design promises as clean a measurement. This year may well be the year in which the problem of neutrino mass is settled. The quantitative answer will be an important tool in uncovering the very poorly

understood relations between lepton families. No deep understanding of the models that unify the forces in nature can be expected without precise knowledge of the masses of neutrinos.

Rare Decays of the Muon

The muon has been the source of one puzzle after another. It was discovered in 1937 in cosmic radiation by Anderson and Neddermeyer and by Street and Stevenson and was assumed to be the meson of Yukawa's theory of the nuclear force.

Yukawa postulated that the nuclear force, with its short range, should be mediated by the exchange of a massive particle, a meson. This differs from the massless photon of the infinite-range electromagnetic force. The muon mass, about 200 times the electron mass, fit Yukawa's theory well.

It was only after World War II ended that measurements of the muon's range in materials were found to be inconsistent with a particle interacting via a strong nuclear force. Discovery of the pion, or pi meson, settled the controversy. To this day, however, casual usage sometimes includes the erroneous phrase "mu meson".

With the resolution of the meson problem, however, the muon had no reason to be. It was simply not necessary. The muon appeared to be, in all known ways, a massive electron with no other distinguishing attributes. A famous quotation of I. I. Rabi summarized the mystery: "The muon, who ordered that?"

This question is none other than the family problem described earlier. Today, the mystery remains, but its complexity has grown. Three generations of fermions exist, and the mysterious relation of the muon to the electron is replicated in the existence of the tau, discovered in 1976 by Martin Perl and collaborators. The three generation scheme is built into the minimal standard model, but there is little insight to guide us to the ultimate number of generations.

Is there a conservation number associated with each family or generation? Are there selection rules or fundamental symmetries that account for the apparent absence of some transitions between these multiplets? Vertical and horizontal transitions between quark states do occur. Processes involving neutrinos connect the lepton generations. Can the pattern of these observed transitions give us a clue as to why we are blessed with this peculiar zoology? Should we look harder for the processes we have not observed? Rabi's question, in its most modern form, is a rich and bewildering one, and many experimental groups have taken up its challenge by pursuing high sensitivity studies of the rare and unobserved reactions that may connect the generations.

With the muon and electron virtual duplicates of each other, it was expected that the heavier muon would decay by simple, *neutrinoless* processes to the electron. Transitions such as $\mu^+ \rightarrow e^+ e^+ e^-$, $\mu^+ \rightarrow e^+ \gamma$, or

Table 1

The additive lepton numbers, their conservation laws, and some of the decays allowed or forbidden by those laws.

Family	Particles	Lepton Number
Electron	e^-, ν_e	$L_e = +1$
	$e^+, \bar{\nu}_e$	$L_e = -1$
Muon	μ^-, ν_μ	$L_\mu = +1$
	$\mu^+, \bar{\nu}_\mu$	$L_\mu = -1$
Tau	τ^-, ν_τ	$L_\tau = +1$
	$\tau^+, \bar{\nu}_\tau$	$L_\tau = -1$

Conservation Laws: $\Sigma L_e = \text{Constant}$, $\Sigma L_\mu = \text{Constant}$, $\Sigma L_\tau = \text{Constant}$

Allowed Decay: $\mu^+ \rightarrow e^+ \nu_e \bar{\nu}_\mu$ Forbidden Decays: $\mu^+ \rightarrow e^+ \gamma$
 $\mu^+ \rightarrow e^+ e^+ e^-$
 $\mu^- Z \rightarrow e^- Z$
 $\mu^- Z \rightarrow e^- (Z-2)$
 $\mu^+ \rightarrow e^+ \bar{\nu}_e \nu_\mu$

$\mu^- Z \rightarrow e^- Z$ (where Z signifies that the interaction is with a nucleus) were expected. Estimates of the rates for these processes using second-order, current-current weak interactions gave results too small to observe. In fact, the results were much smaller than the 1957 limit for the branching ratio for $\mu^+ \rightarrow e^+ \gamma$, which was $< 2 \times 10^{-5}$ (a branching ratio is the ratio of the probability a decay will occur to the probability of the most common decay).

A better early model appeared in 1957 when Schwinger proposed the intermediate vector boson (now called W and observed directly in 1983) as the mediator of the charged-current weak interaction. With this model and under most assumptions, rates larger than the experimental limits were predicted for the three reactions. The failure to observe these decays required a dynamical suppression or a new conservation law. Despite the discussion to follow, the situation today has changed very little. The measured limits are more stringent, though, by many orders of magnitude.

The first proposal for lepton number con-

servation came in 1953. In fact, there have been three different schemes for conserving lepton number. The 1953 Konopinski-Mahmoud scheme cannot accommodate three lepton generations and has not survived. A scheme in which lepton number is conserved by a multiplicative law was proposed in 1961 by Feinberg and Weinberg, but this method is not the favored conservation law. An early experiment with a neutrino detector at the Clinton P. Anderson Meson Physics Facility in Los Alamos (LAMPF) has removed the multiplicative law from favor, and the current experiment to study neutrino-electron scattering, described later in this article, has set even more stringent limits on such a law.

The most favored scheme is additive lepton number conservation, proposed in 1957 by Schwinger, Nishijima, and Bludman. In this scheme, any process must separately conserve the sum of muon number and the sum of electron number. Table 1 shows the assignment of lepton numbers used. The extension to the third lepton flavor, tau, is obvious and natural.

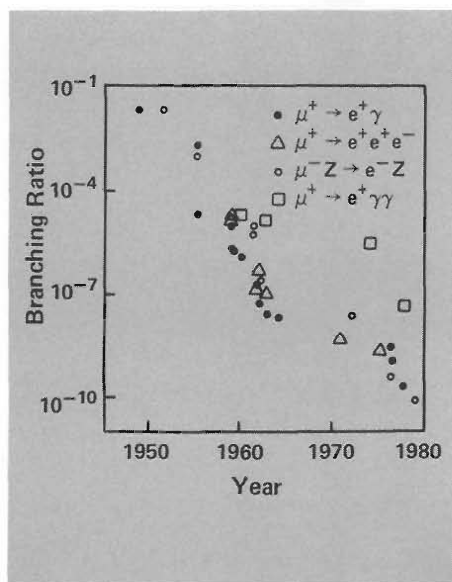


Fig. 4. The progressive drop in the experimentally determined upper limit for the branching ratio of several muon-number violating processes shows a gap in the late 1960s. Essentially, this gap was the result of a belief by particle physicists in lepton number conservation.

These schemes require, as the table hints, a distinct neutrino associated with each lepton. In a 1962 experiment the existence of separate muon and electron neutrinos was confirmed.

With a conservation law firmly entrenched in the minds of physicists, searches for decays that did not conserve lepton number seemed pointless. In a 1963 paper Sherman Frankel observed "Since it now appears that this decay is not lurking just beyond present experimental resolution, any further search . . . seems futile."

In retrospect it can be said that the particle physics community erred. The conclusion stated in the previous paragraph resulted in a nearly complete halt to efforts to detect processes that did not conserve lepton number—and this on the basis of a law postulated without any rigorous or fundamental basis!

It is easy to justify these assertions. Figure 4 shows that the experimental limits on rare decays were not aggressively addressed between 1964 and the late 1970s. This era of inattention ended abruptly when an experimental rumor circulated in 1977—an erroneous report terminated a decade of theoretical prejudice almost overnight! This could not have been the case if lepton conservation was required by fundamental ideas.

In 1977 a group searching for the process $\mu^+ \rightarrow e^+ \gamma$ at the Swiss Institute for Nuclear Research (SIN) became the inadvertent source of a report that the decay had been seen. The experiment, sometimes referred to as the "original SIN" experiment, was an order of magnitude more sensitive than any prior search for this decay and eventually set a limit on the branching ratio of 1.0×10^{-9} . A similar effort at the Canadian meson factory, TRIUMF, produced a limit of 3.6×10^{-9} at about the same time.

The Crystal Box. The extraordinary controversy generated by the "original SIN" report motivated a Los Alamos group to attempt a search for $\mu^+ \rightarrow e^+ \gamma$ with a sensitivity to branching ratios of about 10^{-10} . This experiment was carried out in 1978 and 1979, using several new technologies and a new type of muon beam at LAMPF, and yielded an upper limit of 1.7×10^{-10} (90 per cent confidence level). That result stands as the most sensitive limit on the decay to date but should be surpassed this year by an experiment at LAMPF called the Crystal Box experiment.

This experiment was conceived as the earlier experiment came to an end. By searching for three rare muon decays simultaneously, the experiment would be a major advance in sensitivity and breadth. Several new technologies would be exploited as well as the capabilities of the LAMPF secondary beams.

In any search for a very rare decay, sensitivity is limited by two factors: the total number of candidate decays observed, and any other process that mimics the decay being searched for. The design of an experi-

ment must allow the reliable estimate of the contribution of other processes to a false signal. This is generally done by a Monte-Carlo simulation of these decays that includes taking into account the detector properties.

In the absence of background or a positive signal for the process being studied, the number of seconds the experiment is run translates linearly into experimental sensitivity. However, when a background process is detected, sensitivity is gained only as the square root of the running time. This happens because one must subtract the number of background events from the number of observed events, and the statistical uncertainties in these numbers determine the limit. Generally, when an experiment reaches a level limited by background, it is time to think of an improved detector.

The Crystal Box detector is shown in Fig 5. A beam of muons from the LAMPF accelerator enters on the axis and is stopped in a thin polystyrene target. This beam consists of *surface* muons—a relatively new innovation developed during the 1970s and employed almost immediately at LAMPF and other meson factories.

Normal beams of muons are prepared in a three-step process: a proton beam from the accelerator strikes a target, generating pions; the pions decay in flight, producing muons; finally, the optics in the beam line are adjusted to transport the daughter muons to the experiment while rejecting any remaining pions. A more efficient way to collect low-momentum positive muons involves the use of a beam channel that collects muons from decays of positive pions generated in the target, but the muons collected are from pions that have only just enough momentum to travel from their production point in the target to its surface. Stopped in the surface, their decay produces positive muons of low momentum, near 29 MeV/c (where c is the speed of light). This technique enables experimenters to produce beams of surface muons that can be stopped in a thin experimental target with rates up to a hundred times more than conventional decay beams.

The muons stopped in the target decay virtually 100 per cent of the time by the mode

$$\mu^+ \rightarrow e^+ \nu_e \bar{\nu}_\mu,$$

with a characteristic muon lifetime of 2.2 microseconds. The Crystal Box detector accepts about 50 per cent of these decays and, therefore, must reject the positrons from several hundred thousand ordinary decays occurring each second. At the same time the detector must select those decays that appear to be generated by the processes of interest.

The Crystal Box was designed to simultaneously search for the decay modes

$$\begin{aligned}\mu^+ &\rightarrow e^+ e^+ e^- \\ &\rightarrow e^+ \gamma \\ &\rightarrow e^+ \gamma \gamma.\end{aligned}$$

(Since the Crystal Box does not measure the charge of the particles, we shall not generally distinguish between positrons and electrons in our discussion.)

The *detector properties* necessary for selecting final states from these reactions and rejecting events from ordinary muon decay are:

1. Energy resolution—The candidate decays produce two or three particles whose energies sum to the energy of a muon at rest. The ordinary muon decay and most background processes include particles from several decays or neutrinos that remain undetected but carry away some of the energy. These processes are extremely unlikely to yield the correct energy sum.

2. Momentum resolution—Given energy resolution adequate to accomplish the first requirement, vector momentum resolution requires a measurement of the directions of the particle trajectories. Since muons are stopped in the target, the decays being sought for will have vector momentum sums clustered, within experimental resolution, about zero. Particles from the leading background processes ($\mu^+ \rightarrow e^+ e^+ e^- \nu_e \bar{\nu}_\mu$, $\mu^+ \rightarrow e^+ \gamma \nu_e \bar{\nu}_\mu$, or coincidences of different ordinary muon decays) will tend to have non-

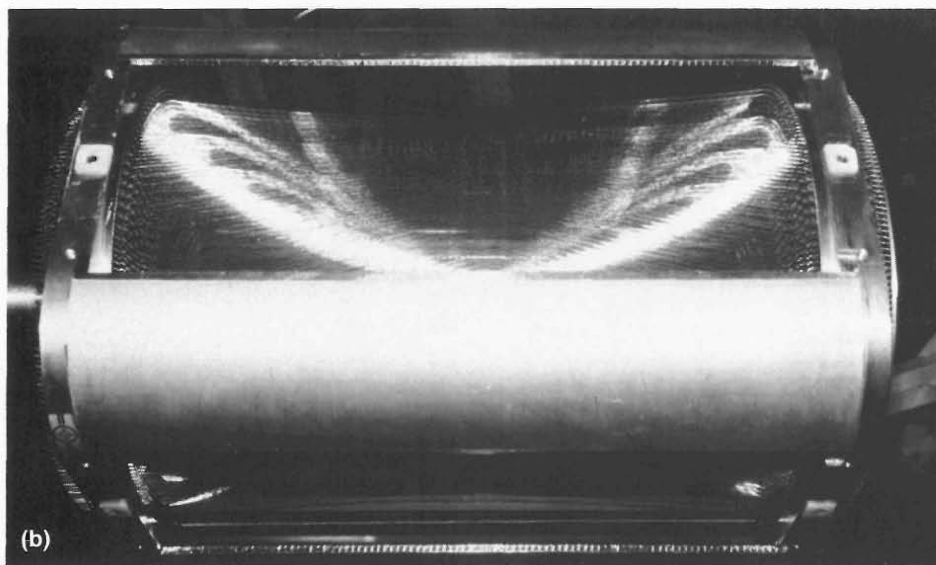
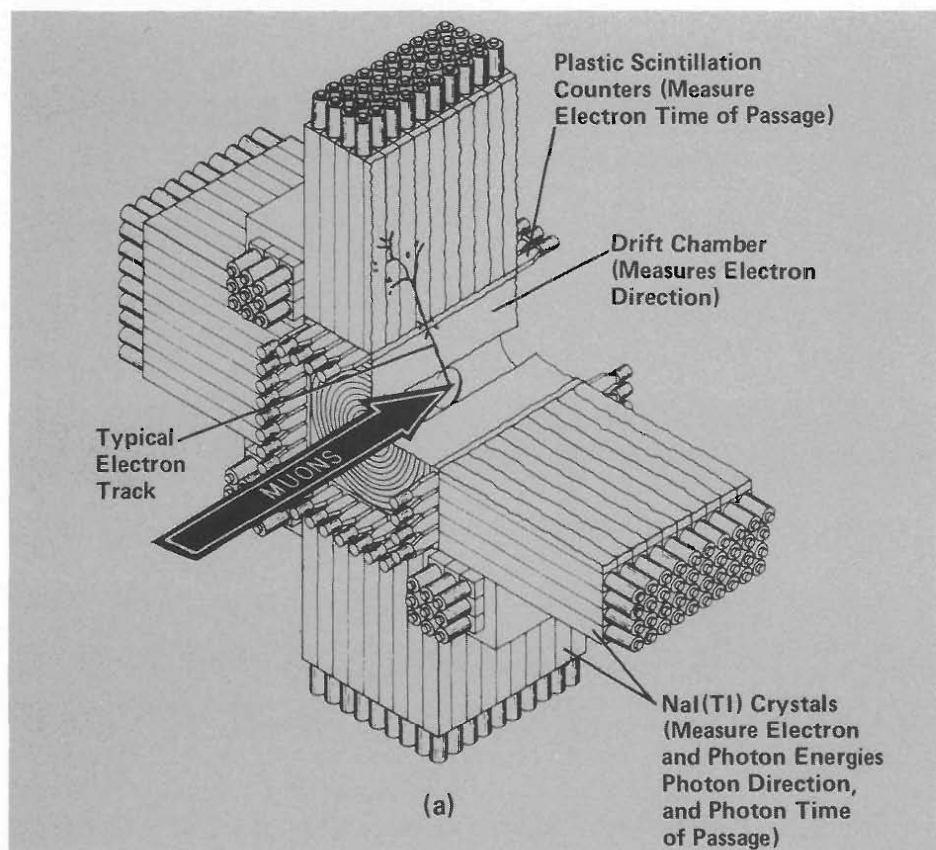
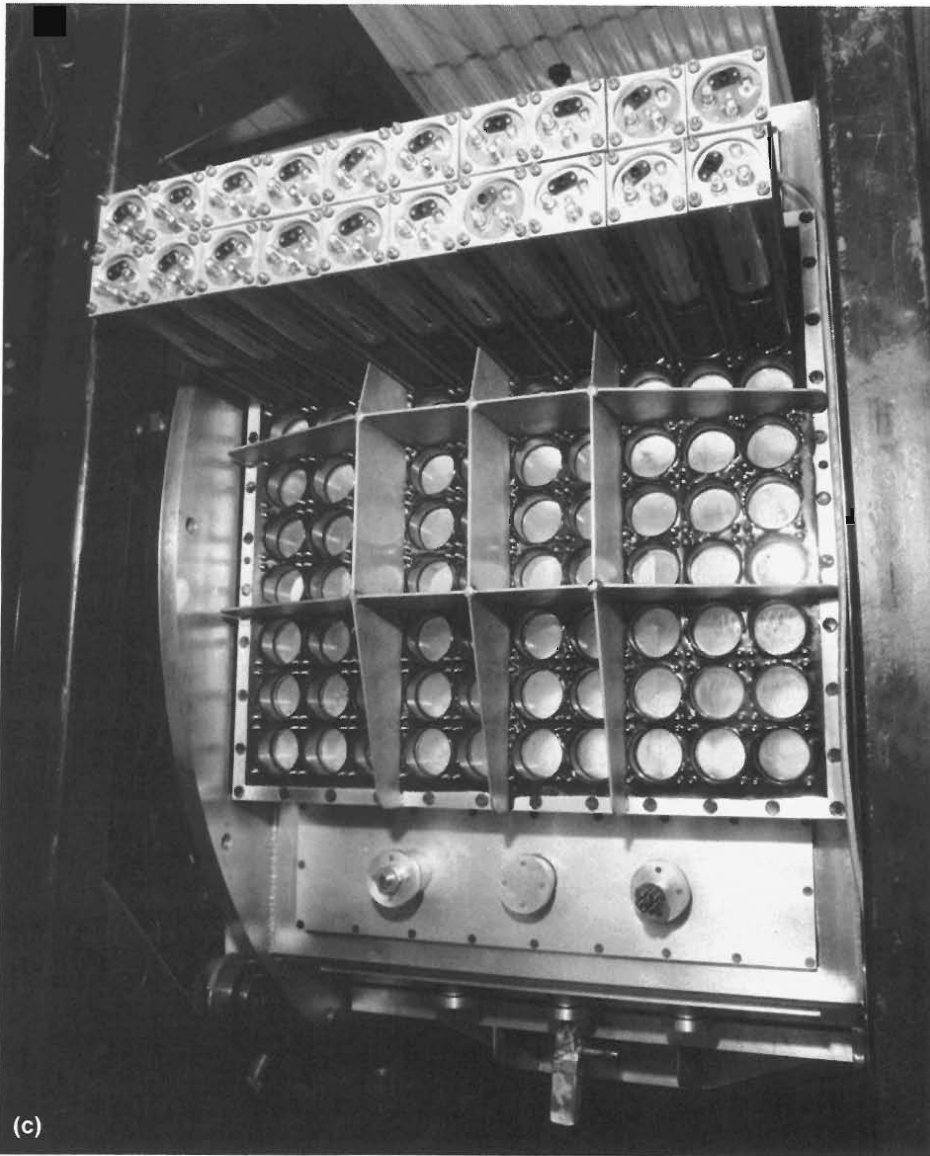


Fig. 5. The Crystal Box detector. (a) A beam of muons enters the detector on axis. Because these are low-momenta surface muons, a thin polystyrene target is able to stop them at rates up to 100 times more than conventional muon beams. The beam intensity is generally chosen to be between 300,000 and 600,000 muons per second with pulses produced at a frequency of 120 hertz and a net duty factor between 6 and 10 per cent. Three kinds of detectors (drift chamber, plastic-scintillation counters, and NaI(Tl) crystals) surround the target. The detector elements are divided into four quadrants, each containing nine rows of crystals with a plastic scintillator in front of each row. This combination of detectors provides information on the energies, times of passage, and directions of the photons and electrons that result from muon decay in the target. The information is used to filter from several hundred thousand ordinary decays per second the perhaps several per second that may be of interest.

A sophisticated calibration and stabilization system was developed to achieve



and maintain the desired energy and time resolution for 4×10^6 seconds of data taking. Before a run starts, a plutonium-beryllium radioactive source is used for electron energy calibration. Also, a liquid hydrogen target is substituted periodically for the experimental target, and the photons emitted in the subsequent pion charge exchange are used for photon energy calibration. During data taking, energy calibration is monitored by a fiber optic flasher system that exposes each photomultiplier channel to a known light pulse. A small number of positrons are accepted from ordinary $\mu^+ \rightarrow e^+ \nu_e \bar{\nu}_\mu$ decays, and the muon decay spectrum cutoff at 52.8 MeV is used as a reference.

(b) The inner detector, the drift chamber, consists of 728 cells in 8 annular rings with about 5000 wires strung to provide the drift cell electrostatic geometry. A 5-axis, computer-controlled milling machine was used to accurately drill the array of 5000 holes in each end plate. These holes, many drilled at angles up to about 10 degrees, had to be located within 0.5 mil so that the chamber wires could be placed accurately enough to achieve a final resolution of about 1 millimeter in measuring the position of a muon decay in the target. The area of the stopping muon spot is about 100 cm^2 . (Photo courtesy Richard Bolton.)

(c) The outer layer of the detector (here shown under construction) contains 396 thallium-doped sodium iodide crystals and achieves an electron and photon energy resolution of 5 to 6 per cent. This layer is highly segmented so that the electromagnetic shower produced by an event is spread among a cluster of crystals. A weighted average of the energy deposition can then be used to localize the interaction point of the photons with a position resolution of about 2 cm.

zero vector sums.

3. Time resolution—Particles from the decay of a single muon are produced simultaneously. A leading source of background for, say $\mu^+ \rightarrow e^+ e^+ e^-$, is three electrons from the decay of three different muons. Such three-body final states are unlikely to occur simultaneously. Precision resolution in the time measurement, significantly better than 1 nanosecond, provides a powerful rejection of those random backgrounds.

4. Position resolution—Decays from a single muon will originate from a single point in the stopping target. Sometimes other processes will add extra particles to an event. The ability to accurately measure the trajectory of each particle in an event is crucial if experimental triggers that have extra tracks or that originate in separate vertices are to be rejected.

These parameters are used to filter measured events. In a sample of 10^{12} muons—the number required to reach sensitivities below the 10^{-11} level—most of this filtering must be done immediately, as the data is recorded. The Crystal Box experiment is exposed to approximately 500,000 muons stopping per second. The experimental “trigger” rate, the rate of decays that satisfy crude requirements, is about 1000 hertz. The detector has been designed with enough intelligence in its hardwired logic circuits to pass events to the data acquisition computer at a rate of less than 10 hertz. In turn, the program in the computer applies more refined filtering conditions so that events are written on magnetic tape at a rate of a few hertz.

Each condition used to narrow down the event sample to those that are real candidates provides a suppression factor. The combined suppression factors must permit the desired sensitivity. The design of the apparatus begins with the required suppressions and applies the necessary technology to achieve them.

A muon that stops in the target and decays by one of the subject decay modes produces only electrons, positrons or photons. The charged particles (hereafter referred to as

electrons) are detected by an 8-layer wire drift chamber (Fig. 5 (b)) immediately surrounding the target. The drift chamber provides track information, pointing back at the origin of the event in the target and forward to the scintillators and crystals to follow. Its resolution and ability to operate in the high flux of electrons from ordinary muon decays in the target have pushed the performance limits of drift chambers; the chamber wires were placed accurately enough to achieve a final resolution of about 1 millimeter (mm) in measuring the position of a muon decay in the target.

Electrons are detected again in the next shell out from the target—a set of 36 plastic scintillation counters surrounding the drift chamber. These counters provide a measurement of the time of passage of the electrons with an accuracy of approximately 350 picoseconds. This accuracy is extraordinary for counters of the dimensions required (70 cm long by 6 cm wide by 1 cm thick) but is crucial to suppressing the random trigger background for the $\mu^+ \rightarrow e^+ e^+ e^-$ reaction. This performance is achieved by using two photomultiplier tubes, one at each end of the scintillator, and two special electronic timing circuits developed by the collaborators.

The electrons and photons that pass through the plastic scintillators deposit their energy in the next and outermost layer of the detector, a 396-crystal array of thallium-doped sodium iodide crystals. These crystals, acting as scintillators, provide fast precision measurement of both electron and photon energy (providing the energy and momentum filtering described earlier) and localize the interaction point of the photons with a position resolution of about 2 cm. The use of such large, highly segmented arrays of inorganic scintillator crystals was pioneered in high-energy physics in the late 1970's by the Crystal Ball detector at the Stanford Linear Accelerator Center. This technology is now widespread in particle physics research, with detectors planned that involve as many as 12,000 crystals.

The sodium iodide array also provides accurate time measurements on the photons.

A fast photomultiplier tube and electronics with special pulse shaping, amplification, and a custom-tailored, constant-fraction timing discriminator were melded into a system that gives subnanosecond accuracy.

The major detector elements—the drift chamber, plastic scintillators and sodium iodide crystals—are used in logical combinations to select events that may be of interest. A $\mu^+ \rightarrow e^+ e^+ e^-$ event is selected when three or more non-adjacent plastic scintillators are triggered and energy deposit occurs in the sodium iodide rows behind them. The special circuits developed for the scintillators are used for this selection: one high-speed circuit insures that the three or more triggers are coincident within a very tight time interval (approximately 5 nanoseconds), the second circuit requires the three or more hits to be in non-adjacent counters. The last requirement suppresses events in which low momentum radiative daughters trigger adjacent counters or when an electron crosses the crack between two counters.

An even more sophisticated trigger processor was constructed to insure that the three particles triggering the apparatus conform to a topology consistent with a three-body decay of a particle at rest. Thus, a pattern of tracks that, say, necessarily has net momentum in one direction (Fig. 6 (a)) is rejected, but a pattern with the requisite symmetry (Fig. 6 (b)) is accepted. This "geometry box" is an array of programmable read-only-memory circuits loaded with all legal hit patterns as determined by a Monte-Carlo simulation of the $\mu^+ \rightarrow e^+ e^+ e^-$ experiment.

Finally, the total energy deposited in the sodium iodide must be, within the real-time energy resolution, consistent with the rest energy of a muon.

The $\mu^+ \rightarrow e^+ \gamma$ and $\mu^+ \rightarrow e^+ \gamma \gamma$ reactions are selected by combining an identified electron (a plastic scintillator counter triggered coincident with sodium iodide signals) and one or more photons (a sodium iodide signal triggered with no count in the plastic scintillator in front of it). Also, these events must be in the appropriate geometric pattern (for example, directly opposite each other for μ^+

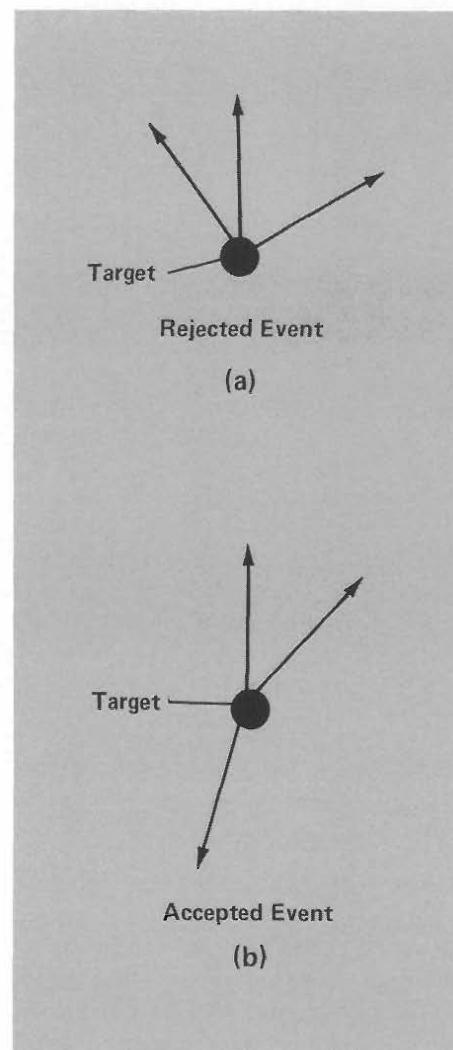


Fig. 6. (a) A pattern of tracks with net momentum is not consistent with the neutrinoless decay of a muon at rest, and such an event will be rejected, whereas an event with a pattern such as the one in (b) will be accepted.

$\rightarrow e^+ \gamma$) and have the correct energy balance.

The Crystal Box should report limits in the 10^{-11} range on the three reactions of interest this calendar year. It will also be used during the next year in a search for the $\pi^0 \rightarrow \gamma \gamma \gamma$ decay, which violates charge conjugation invariance. A search for only the $\mu^+ \rightarrow e^+ e^+ e^-$

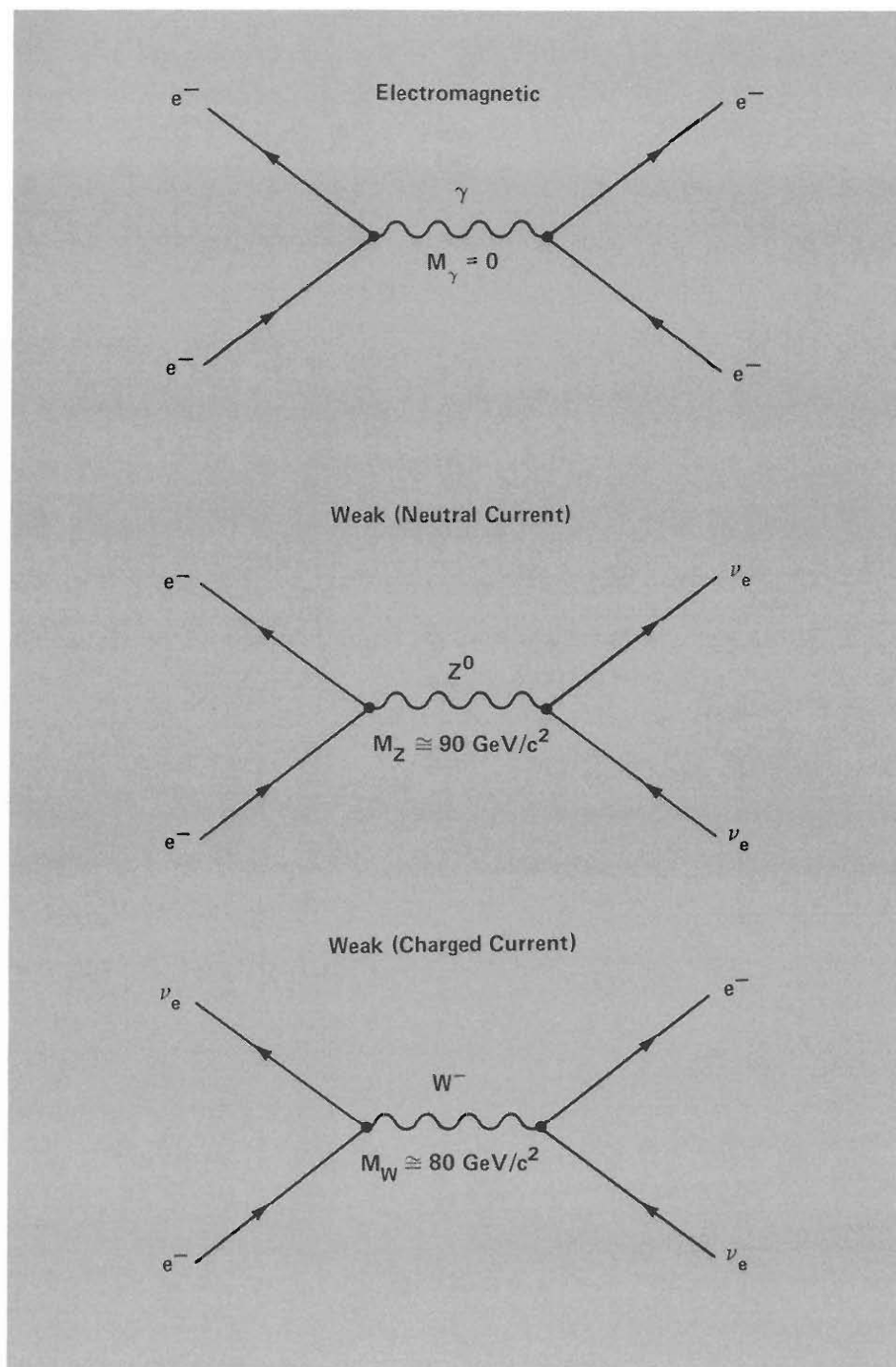


Fig. 7. Examples of the electromagnetic and weak interactions in quantum field theory.

process is being carried out at the Swiss Institute for Nuclear Research with an ultimate sensitivity of 10^{-12} available in the next year.

A third LAMPF $\mu^+ \rightarrow e^+ \gamma$ experiment is planned after the Crystal Box experiment. With present meson factory beams and foreseeable detector technology, this next generation experiment may well be the final round.

Neutrino-Electron Scattering

The unification of the electromagnetic and weak interactions is a treatment of physical processes described by the exchange of three fundamental bosons. The exchange of a photon yields an electromagnetic current, and the W^\pm and Z^0 bosons are exchanged in interactions classified as charged and neutral weak currents, respectively. Figure 7 illustrates how quantum field theory represents these processes.

A traditional method of probing electroweak unification in the standard model has been to determine the precise onset of weak effects in an interaction that is otherwise electromagnetic. Especially important are experiments—with polarized electron scattering at fixed target accelerators and more recent studies at electron-positron colliders—that probe the *interference* between the amplitudes of the electromagnetic and neutral-current weak interactions. Interference effects may be easier to observe than direct measurement of the small amplitudes of the weak interaction.

An Irvine-Los Alamos-Maryland team is conducting a unique and novel search for another interference. They have set out to probe the *purely* weak interference between the amplitudes of the charged and neutral currents. In the same way that electron scattering experiments search for interference between photon and Z^0 boson interactions, the Los Alamos based experiment is searching for the interference between charged-current W interactions and neutral-current Z^0 interactions.

This experiment is attempting a unique

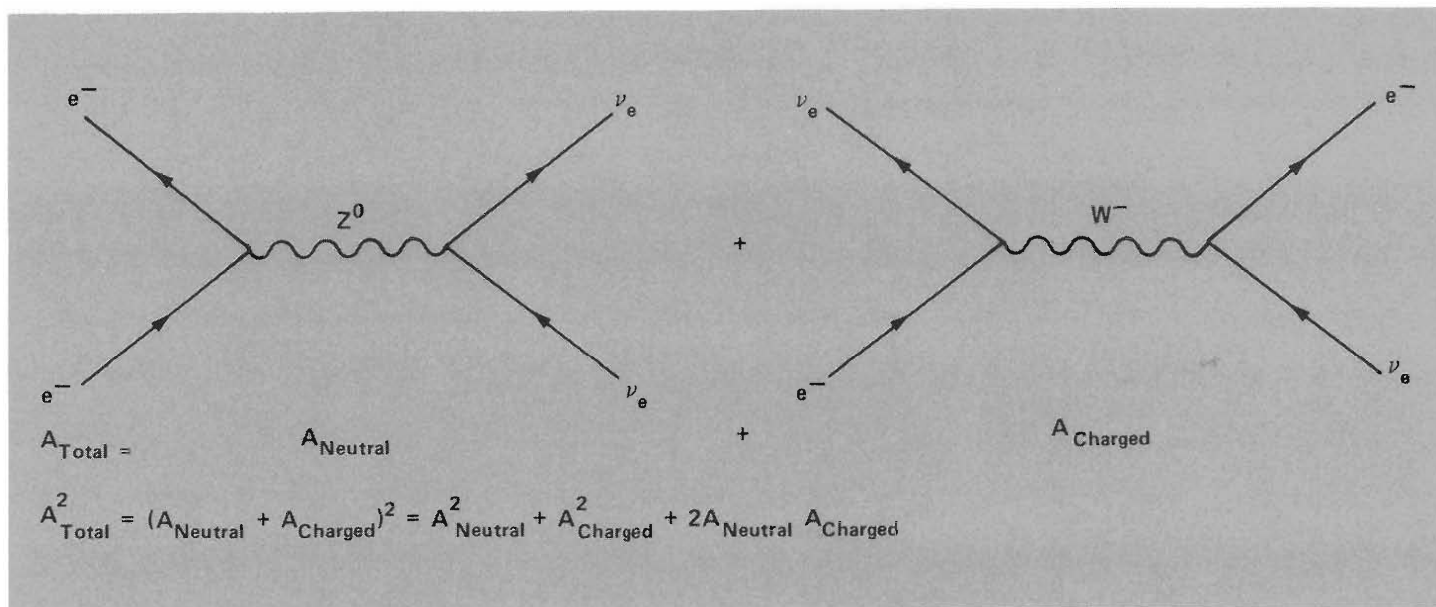


Fig. 8. The interaction between an electron and its neutrino can take place via either the neutral current (with a Z^0) or the charged current (with a W^-), which results in an interference term ($2A_{\text{Neutral}}A_{\text{Charged}}$) in the expression for the

square of the total amplitude A_{Total} . An experiment at LAMPF will probe this purely weak interference by studying ν_e -electron scattering.

measurement because Los Alamos is currently the only laboratory in the world with the requisite source of electron neutrinos. Moreover, the experiment gains importance from the fact that comparatively little is known about the physics of the Z^0 relative to that of the W .

The measurement is a simple variation on the electron-electron scattering experiments. To substitute the W current for the electromagnetic current, the experimenters substitute the electron neutrino ν_e as the projectile and set out to measure the frequency of electron-neutrino elastic scattering from electrons. While this is conceptually simple, it is, in fact, technically quite difficult. The experiment must yield a sufficiently precise measure of the frequency of these scatters to separate out theoretical predictions made with different assumptions. To illustrate how the experiment tests the standard model, we must examine the nature of the model's predictions for ν_e - e scattering.

Electroweak theory obeys the group structure $SU(2) \times U(1)$. The $SU(2)$ group has three generators, W^+ , W^- , and W^3 , which are the charged and neutral vector bosons identified with the gauge fields. The $U(1)$ group has a single neutral boson generator B . The familiar phenomenological neutral photon field is constructed from the linear combination

$$A_\mu = W^3 \sin \theta_W + B \cos \theta_W,$$

(where θ_W is the Weinberg angle, a measure of the ratio of the contributions of the weak and the electromagnetic forces to the total interaction). The phenomenological neutral current carried by the Z^0 is similarly constructed from

$$Z^0 = W^3 \cos \theta_W - B \sin \theta_W.$$

In the standard model the process

$$\nu_e + e^- \rightarrow \nu_e + e^-$$

can take place by the exchange of either the neutral-current boson Z^0 or the charged-current boson W^- (Fig. 8), resulting in the usual interference term for the probability of a process that can take place in either of two ways. The question then is what form will this interference take.

All models of the weak interaction that are currently considered viable predict a *negative, or destructive*, interference term. A model that can produce *constructive* interference is one that includes additional neutral gauge bosons beyond the Z^0 . Thus, the observation of a ν_e - e scattering cross section consistent with constructive interference would indicate a phenomenal change in our picture of electroweak physics. Since the common Z^0 with about the predicted mass was directly observed only last year, and since higher mass regions will be accessible during this decade, such a result would set off a vigorous search by the particle physics community.

How will the traditional low-energy theory

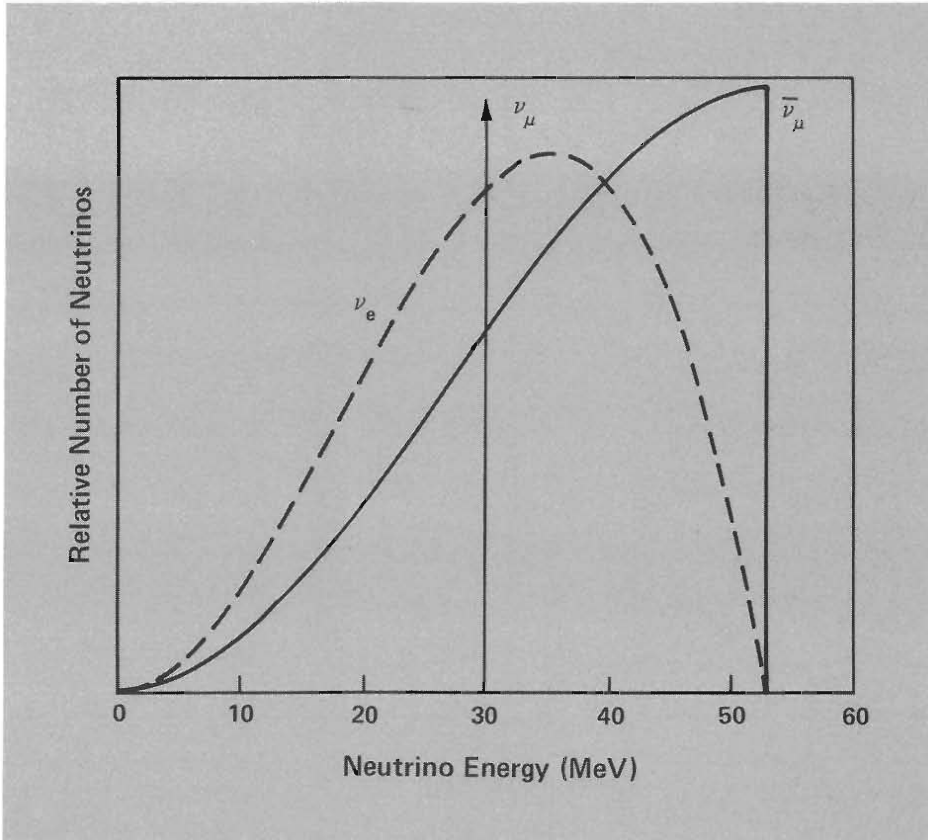


Fig. 9. The energy spectra for the three types of neutrinos that result from the decay of a positive pion ($\pi^+ \rightarrow \mu^+ + \nu_\mu$, $\mu^+ \rightarrow e^+ + \nu_e + \bar{\nu}_\mu$).

of weak interactions (apparently governed by $V - A$ currents) mesh with future observations at higher energies? The standard model prediction, which contains negative interference, is that the cross section for $\nu_e - e$ elastic scattering should be about 60 per cent of the cross section in the traditional $V - A$ theory. The LAMPF experiment must measure the cross section with an accuracy of about 15 per cent to be able to detect the lower rate that would occur in the presence of interference and thus be able to determine whether interference effects are present or not.

In addition, the magnitude of the interference is a function of $\sin^2\theta_W$, and a precise measurement of the interference constitutes a measurement of this factor. In fact, it is

statistically more efficient to do this with a neutral current process because the charged current contains $\sin^2\theta_W$ (≈ 0.25) summed with unity, whereas for the neutral current the leading term is $\sin^2\theta_W$.

The Experiments. The LAMPF proton beam ends in a thick beam stop where pions (π^+) are produced. These pions decay by the process

$$\begin{aligned} \pi^+ &\rightarrow \mu^+ + \nu_\mu \\ &\quad \downarrow \\ &\quad e^+ + \nu_e + \bar{\nu}_\mu, \end{aligned}$$

yielding three types of neutrinos exiting the beam stop. The ν_e and $\bar{\nu}_\mu$ are each produced with a continuous spectrum (Fig. 9) typical of muon decay, whereas the ν_μ spectrum, the

result of a two-body decay, is monoenergetic with an energy at about 30 MeV. The $\bar{\nu}_\mu$ spectrum has a cutoff energy at about 53 MeV, and the ν_e spectrum peaks around 35 or 40 MeV then falls off, also at about 53 MeV. These three particles are the source of many possible measurements.

The primary goal is the study of the $\nu_e - e$ elastic scattering already discussed. The detector, which we shall describe in more detail shortly, must detect electrons characteristic of the elastic scattering, that is, they should have energies between 0 and 53 MeV and lie within about 15 degrees of the forward direction (the tracks must point back to the neutrino source).

Also, by selecting events with electrons below 35 MeV, the group will search for the first observation of an exclusive neutrino-induced nuclear transition. The process

$$\nu_e + {}^{12}\text{C} \rightarrow e^- + {}^{12}\text{N}$$

would produce electrons with less than 35 MeV energy that lie predominantly outside the angular region for the elastic scattering events.

Another important physics goal, neutrino oscillations, can be addressed simultaneously. A process, called an "appearance," in which the $\bar{\nu}_\mu$ species disappears from the beam and $\bar{\nu}_e$ appears, can be probed by searching for the presence of $\bar{\nu}_e$ in the beam. This type of neutrino does not exist in the original neutrino source, so its presence downstream could be evidence for the $\bar{\nu}_\mu - \bar{\nu}_e$ oscillation. The experimental signature for such a process is the presence of isotropic single positrons produced by the reaction

$$\bar{\nu}_e + p \rightarrow n + e^+,$$

combined with a selection in energy of more than 35 MeV, which can be used to isolate these candidate events from the nuclear transition process discussed above.

In all three of the processes studied, the technical problem to be solved is the separation of the desired events from competing

background processes. The properties of the detector (Fig. 10) needed to do this include:

1. Passive shielding—Lead, iron, and concrete are used to absorb charged and neutral cosmic ray particles entering the detector volume. However, the shield is not thick enough to insure that events seen in the inner detector come only from neutrinos entering the detector and not from residual cosmic ray backgrounds. The outer shield merely reduces the flux, consisting mainly of muons and hadrons from cosmic rays and of neutrons from the LAMPF beam stop.

The LAMPF beam is on between 6 and 10 per cent of each second so that the periods between pulses will provide an important normalizing measurement indicating how well the passive shielding works.

2. Active anti-coincidence shield—This multilayer device is an active detector that surrounds the inner detector and serves many purposes. For example, muons from cosmic rays that penetrate the passive shield are detected here by being coincident in time with an inner detector trigger. This allows the rejection of these “prompt” muons, with less than one muon in 10^4 surviving the rejection. Data acquisition electronics that store the history of the anti-coincidence shield for 32 microseconds prior to an inner detector trigger serve an even more complex purpose. This information is used to reject any inner detector electrons coming from a muon that stopped in the outer shield and that took up to 32 microseconds to decay. The mean muon lifetime is only 2.2 microseconds, so this is a very satisfactory way to reject such events.

3. Inner converter—Photons penetrating the anti-coincidence layer, produced perhaps by cosmic rays or particles associated with the beam, strike an additional layer of steel and are either absorbed or converted into electronic showers that are seen as tracks connected to the edge of the inner detector. Such events are discarded in the data analysis.

4. Inner detector—This module’s primary role is to measure the trajectory and energy deposition of electrons and other charged

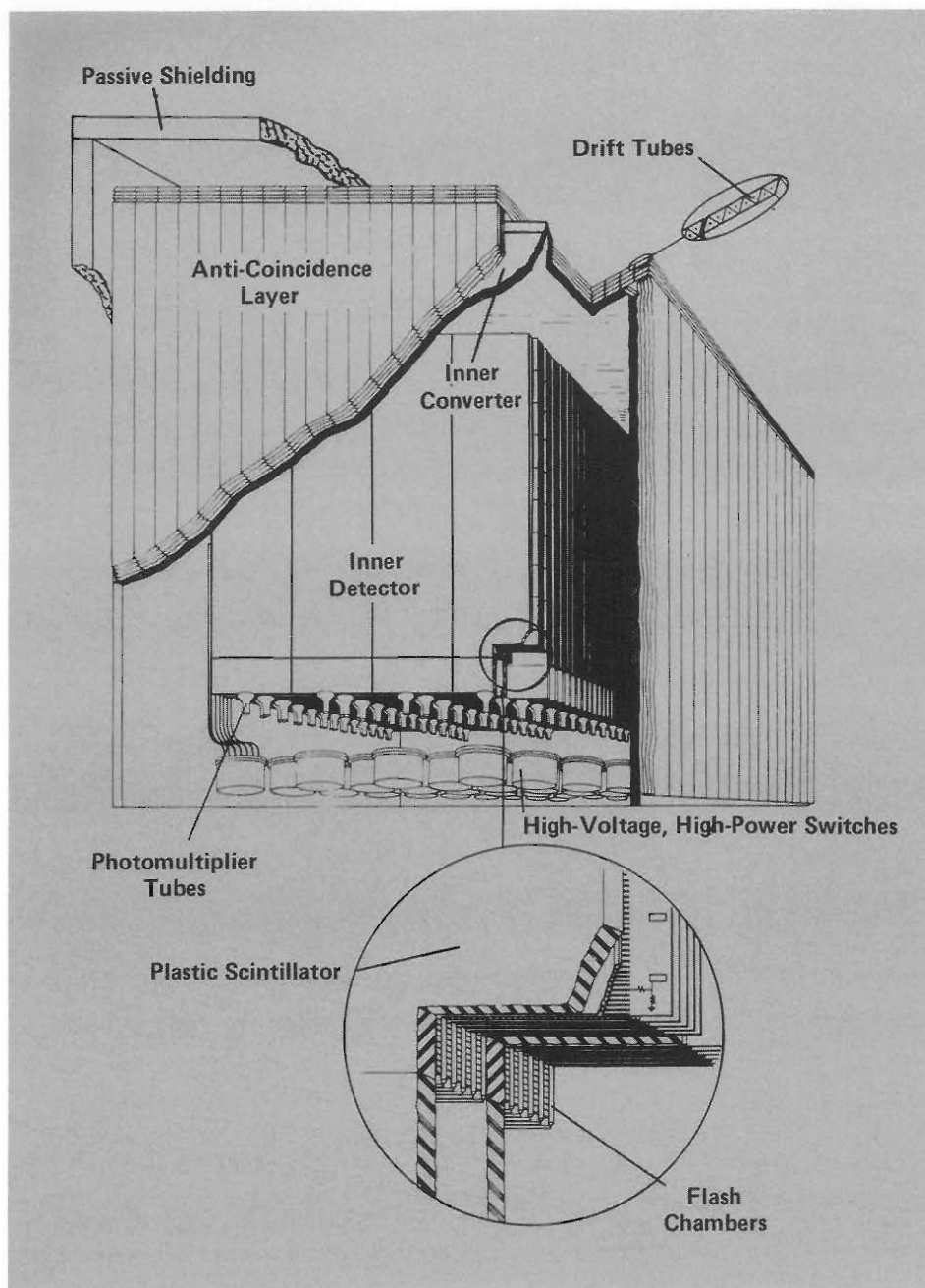


Fig. 10. The detector for the neutrino-electron scattering experiments. The outer layer of passive shielding (mainly steel) cuts down the flux of neutral solar particles.

The anti-coincidence shield rejects muons from cosmic rays and electrons coming from the decay of muons stopped in the outer shield. It consists of four layers of drift tubes, totaling 603 counters, each 6 meters long. A total of 4824 wires provides a fine-grained, highly effective screen, with an inefficiency (and therefore a suppression) of 2×10^{-5} .

Another steel layer, the inner converter, is used to reject photons from cosmic rays or other particles associated with the beam.

The inner detector consists of 10 tons of plastic scintillators interleaved with 4.5 tons of tracking chambers. The plastic scintillators sample the electron energy every 10 layers of track chamber. There are 160 counters, each 75 cm by 300 cm by 2.5 cm thick, and they measure the energy to about 10 per cent accuracy. The track chambers are a classic technology: they are flash chambers that behave like neon lights when struck by an ionizing particle, discharging in a luminous and climactic way. There are a phenomenal 208,000 flash tubes in the detector, and they measure the electron tracks and sort them into angular bins about 7 degrees wide.

particles. Electron tracks are the signature of the desired neutrino reactions, but recoil protons generated by neutrons from the beam stop and from cosmic rays must also be detected and filtered out in the data analysis. The inner detector contains layers of plastic scintillators that sample the particle energy deposited along its path for particle identification and also provide a calorimetric measurement of the total energy. Trajectory measurement is provided by a compact system of flash chambers interleaved with the plastic scintillators.

When this detector is turned on, it counts about 10^8 raw events per day, mostly from cosmic rays. To illustrate the selectivity required of this experiment, a recent data run of a few months is expected to produce somewhat less than 50 ν_e - e elastic scattering events.

This highly segmented detector is necessarily extremely compact. The neutrino flux produced in the beam stop is emitted in all directions and therefore has an intensity that falls off inversely with the square of the distance. Thus there was a strong design premium for developing a compact, dense detector and placing it as close to the source as feasible.

The detector is now running around the clock, even when the LAMPF beam is off (to pin down background processes). The data already taken include many ν_e - e events that are being reported, as are preliminary results on lepton number conservation and neutrino oscillations. Data taken with additional neutron shielding during the next year or two are expected to provide the precision test of the standard model that the experimenters seek.

Beyond this effort, the beginnings of a much larger and ambitious neutrino program at Los Alamos are evident. A group (Los Alamos; University of New Mexico; Temple University; University of California, Los Angeles and Riverside; Valparaiso University; University of Texas) working in a new LAMPF beam line are mounting the prototype for a much larger fine-grained neutrino detector. Currently, a focused beam

source of neutrinos is being developed that will eventually employ a rapidly pulsed "horn" to focus pions that decay to neutrinos. This development will be used to provide neutrinos for a major new detector. The group is not content to work merely on developing the facility but is using a preliminary detector to measure some key cross sections and set new limits on neutrino oscillations as well.

Another group (Ohio State, Louisiana State, Argonne, California Institute of Technology, Los Alamos) is assembling the first components of an aggressive effort to search for the $\bar{\nu}_e$ appearance mode. Other physicists at the laboratory are preparing a solar neutrino initiative.

The exciting field of neutrino research, begun by Los Alamos scientists, is clearly entering a golden period.

Precision Studies of Normal Muon Decay

The measurement of the electron energy spectrum and angular distribution from ordinary muon decay,

$$\mu \rightarrow e + \bar{\nu}_e + \nu_\mu,$$

is one of the most fundamental in particle physics in that it is the best way to determine the constants of the weak interaction. These studies have led to limits on the $V-A$ character of the theory.

The spectrum of ordinary muon decay may be precisely calculated from the standard model. Built into the minimal standard model—consistent with the idea that everything in the model must be required by measurements—are the assumptions that neutrinos are massless and the only interactions that enter are of vector and axial vector form (that is, $V-A$, or equal magnitude and opposite sign). Lepton flavor conservation is also taken to be exact.

This $V-A$ structure of the weak interaction can be tested by precise measurements of the electron spectrum from ordinary

muon decay. The spectrum is characterized (to first order in m_e/m_μ and integrated over the electron polarization) by

$$\begin{aligned} \frac{dN}{x^2 dx d(\cos \theta)} &\propto (3-2x) \\ &+ \left(\frac{4}{3}\rho - 1\right)(4x-3) \\ &+ 12 \frac{m_e}{m_\mu} \frac{(1-x)}{x^2} \eta + \left[(2x-1) + \left(\frac{4}{3}\delta - 1\right)(4x-3)\right] \xi \mathbf{P}_\mu \cos \theta, \end{aligned}$$

where m_e is the electron mass, θ is the angle of emission of the electron with respect to the muon polarization vector \mathbf{P}_μ , m_μ is the muon mass, and x is the reduced electron energy ($x = 2E/m_\mu$ where E is the electron energy). The Michel parameters ρ , η , ξ , δ characterize the spectrum.

The standard model predicts that

$$\rho = \delta = 3/4, \quad \xi = 1, \quad \text{and} \quad \eta = 0.$$

One can also measure several parameters characterizing the longitudinal polarization of the electron and its two transverse components. Table 2 gives the current world average values for the Michel parameters. These data have been used to place limits on the weak interaction coupling constants, as shown in Table 3. As can be seen, the current limits allow up to a 30 per cent admixture of something other than a pure $V-A$ structure. Other analyses, with other model-dependent assumptions, set the limit below 10 per cent.

One of the extensions of the minimal standard model is a theory with left-right symmetry. The gauge symmetry group that embodies the left-handed symmetry would be joined by one for right-handed symmetry, and the charged-current bosons W^+ and W^- would be expanded in terms of a symmetric combination of fields W_L and W_R . Such an

extension is important from a theoretical standpoint for several reasons. First, it restores parity conservation as a high-energy symmetry of the weak interaction. The well-known observation of parity violation in weak processes would then be relegated to the status of a low-energy phenomenon due to the fact that the mass of the right-handed W is much larger than that of the left-handed W . Each lepton generation would probably require two neutrinos, a light left-handed one and a very heavy right-handed member.

The dominance of the left-handed charged current at presently accessible energies would be due to a very large mass for W_R , but the $W_L - W_R$ mass splitting would still be small on the scale of the grand unification mass M_X . Thus the precision study of a weak decay such as ordinary muon decay or nucleon beta decay can be used to set a limit on the left-right symmetry of the weak interaction.

With such plums as the $V-A$ nature of the weak interaction and the existence of right-handed W bosons accessible to such precision studies, it is not surprising that several experimental teams at meson factories are carrying out a variety of studies of ordinary muon decay. One team working at the Canadian facility TRIUMF has already collected data and set a lower limit of 380 GeV on the mass of the right-handed W . This was done with a muon beam of only a few MeV!

The Time Projection Chamber. A Los Alamos - University of Chicago-NRC Canada collaboration is carrying out a particularly comprehensive and sensitive study of the muon decay spectrum using a novel and elaborate device known as a time projection chamber (TPC).

The TPC (Fig. 11) is a very large volume drift chamber. In a conventional drift chamber, an array of wires at carefully determined potentials collects the ionization left in a gas by a passing charged particle. The time of arrival of the packet of ionization in the cell near each wire is used to calculate the path of the particle through the cell. The gas

Table 2

Theoretical and experimental values for the weak-interaction Michel parameters.

Michel Parameter	$V-A$ Prediction	Current Value	Expected Los Alamos Accuracy
ρ	$\frac{3}{4}$	0.752 ± 0.003	± 0.00023
η	0	-0.12 ± 0.21	± 0.0061
ξ	1	0.972 ± 0.014	± 0.001
δ	$\frac{3}{4}$	0.755 ± 0.008	± 0.00064

Table 3

Experimental limits on the weak-interaction coupling constants, including the expected limit for the Los Alamos Experiment.

Constant	Present Limit	Expected Limit
Axial Vector	$0.76 < g_A < 1.20$	$0.988 < g_A < 1.052$
Tensor	$g_T < 0.28$	$g_T < 0.027$
Scalar	$g_S < 0.33$	$g_S < 0.048$
Pseudo Scalar	$g_P < 0.33$	$g_T < 0.048$
Vecto-axial Vector Phase	$\phi_{VA} = 180^\circ \pm 15^\circ$	$\phi_{VA} = 180^\circ \pm 2.6^\circ$

and the field in the cell are chosen so that the ionization drifts at a constant terminal velocity. Thus the calculation of the position from the drift time can be done accurately. Many drift chambers provide coordinate measurements accurate to less than 100 micrometers.

On the other hand, a TPC uses the same drift velocity phenomenon but employs it in a large volume with no wires in the sensitive region. The path of ionization drifts en masse under the influence of an electric field along the axis of the chamber. The ionization is collected on a series of electrodes, called

pads, on the chamber endcaps, providing precision measurement of trajectory charge and energy. The pad signal also gives a time measurement, relative to the event trigger, that can be used to reconstruct the spatial coordinate of each point on the trajectory.

The TPC in the Los Alamos experiment is placed in a magnetic field sufficiently strong that the decay electrons, whose energies range up to about 53 MeV, follow helical paths. The magnetic field is accurate enough to make absolute momentum measurements of the decay electrons.

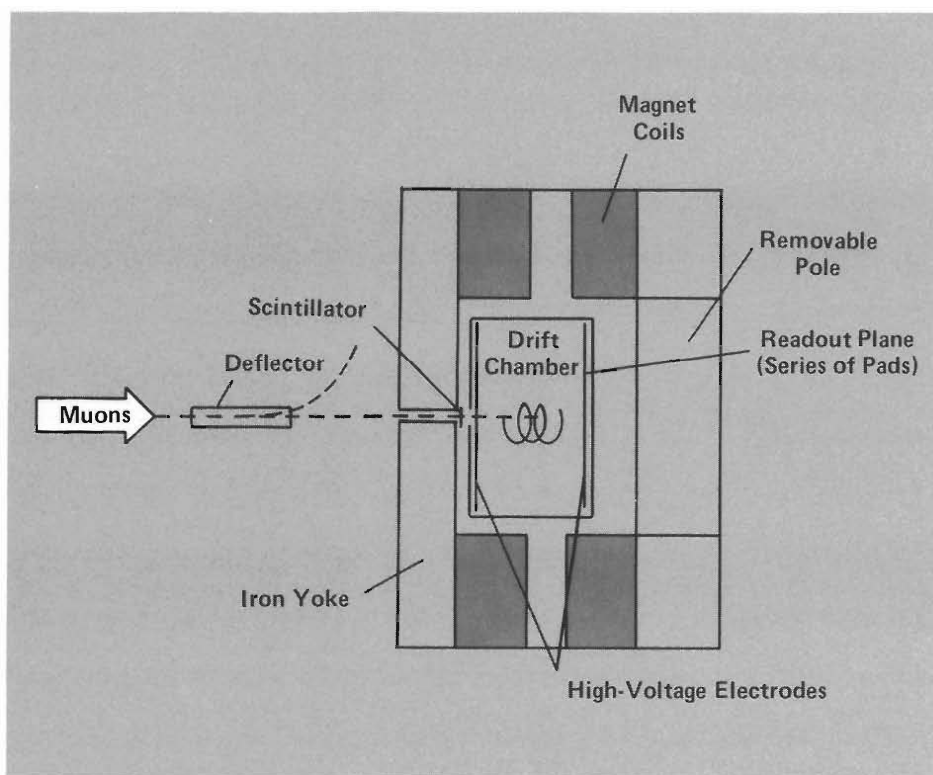


Fig. 11. The time projection chamber (TPC), a device to study the muon decay spectrum. A beam of muons from LAMPF enters the TPC via a 2-inch beam pipe that extends through the magnet pole parallel to the magnetic field direction. Before entering the chamber, the muons pass through a 10-mil thick scintillator that serves as a muon detector. The scintillator is viewed, via fiber optic light guides, by two photomultiplier tubes located outside the magnet. The thresholds for the discriminators on these photomultiplier channels are adjusted to produce a coincidence for the more heavily ionizing muons while the minimum-ionizing beam electrons are ignored. A deflector located in the beam line 2 meters upstream of the magnet produces a region of crossed electric and magnetic fields through which the beam passes. This device acts first as a beam separator, purifying the muon flux—in particular, reducing the number of electrons in the beam from about 200 to about 1.5 for every muon. The device also acts as a deflector, keeping additional particles out of the chamber by switching off the electric field once a muon has been observed entering the detector. The magnetic field in this detector is provided by an iron-enclosed solenoid, with the maximum field in the current arrangement being 6.6 kilogauss. The field has been carefully measured and found to be uniform to better than 0.6 per cent within the entire TPC-sensitive volume of 52 cm in length by 122 cm in diameter. The TPC readout, on the chamber endcaps, consists of 21 identical modules, each of which has 15 sense wires and 255 pads arranged under the sense wires in rows of 17 pads each. The sense wires provide the high field gradient necessary for gas amplification of the track ionization. The 21 modules are arranged to cover most of the 122-centimeter diameter of the chamber.

A beam of muons from LAMPF passes first through a device that acts as a beam separator, purifying the muon flux (especially of electrons, which are reduced by this device from an electron-to-muon ratio of 200:1 to about 3:2). The device also acts as a deflector, keeping additional particles from entering the chamber once a muon is inside. With a proper choice of beam intensity, only one muon is allowed in the TPC at a time. Next the beam passes through a 10-mil thick scintillator (serving both as a muon detector and a device used to reject events caused by the remaining beam electrons) and continues into the TPC along a line parallel to the magnetic field direction.

The requirement for an event to be triggered is that one muon enters the TPC during the LAMPF beam pulse and stops in the central 10 cm of the drift region. The entering muon is detected by a signal coincidence from photomultipliers attached to the 10-mil scintillator (this signal operates the deflector that keeps other muons out). The scintillator signal must also be coincident—including a delay that corresponds to the drift time from the central 10 cm of the TPC—with a high level signal from any of the central wires of the TPC. If no delayed coincidence occurs, indicating that the muon did not penetrate far enough into the TPC, or a high level output is detected before the selected time window, indicating that the muon penetrated too far, the event is rejected and all electronics are reset. Then 250 microseconds later (to allow for complete clearing of all tracks in the TPC) the beam is allowed to re-enter for another attempt. The event is also rejected if a second muon enters the TPC during the 200-nanosecond period required to turn off the deflector electric field.

If the event is accepted, the computer reads 20 microseconds of stored data. This corresponds to five muon decay lifetimes plus the 9 microseconds it takes for a track to drift the full length of the TPC.

The experiment is expected to collect about 10^8 muon decay events, at a trigger rate of 120 events per second, during the next year. Preliminary data have already been

taken, showing that the key resolution for electron momentum falls in the target range, namely $\Delta p/p$ is 0.7 per cent averaged over the entire spectrum. Figure 12 shows one of the elegant helical tracks obtained in these early runs.

Ultimately, this experiment will be able to improve upon the four parameters shown in Table 2, although the initial emphasis will be on ρ . In the context of left-right symmetric models, an improved measurement of ρ will place a new limit on the allowed mixing angle between W_R and W_L that is almost independent of the mass of the W_R .

Summary

The particle physics community is aggressively pursuing research that will lead to verification or elaboration of the minimal standard model. Most of the world-wide activity is centered at the high-energy colliding beam facilities, and the last few years have yielded a bountiful harvest of new results, including the direct observation of the W^\pm and Z^0 bosons and the top quark. Many of the key measurements of the 1980s are likely to be made at the medium-energy facilities, such as LAMPF, or in experiments far from accelerators, deep underground and at reactors, where studies of proton decay, solar

neutrino physics, neutrino oscillations, tritium beta decay, and other bellwether research is being carried out.

The program of fundamental particle physics research at Los Alamos is making aggressive use of our unique facilities to search higher mass scales, to push current theory to its limits, and to provide some of the key measurements available only at lower energies. Extensions to our physical theories may well be driven by such work. The observation of lepton flavor non-conservation, a neutrino mass, the absence of interference between the charged and neutral weak currents, of right-handed charged

current effects in muon decay, or neutrino oscillations would set off revolutionary changes in the accepted dogma.

The program at Los Alamos is not a static one, and many ambitious initiatives are being pursued. Further work on rare muon decays and neutrino scattering are proposed. Studies deep underground of solar neutrino physics and other fields are included in a proposed national facility for underground physics. Studies of rare kaon decays and a proposed major addition to the LAMPF facility, LAMPF II, herald a grand era of kaon, neutrino, and antiproton physics on our mesa tops. ■

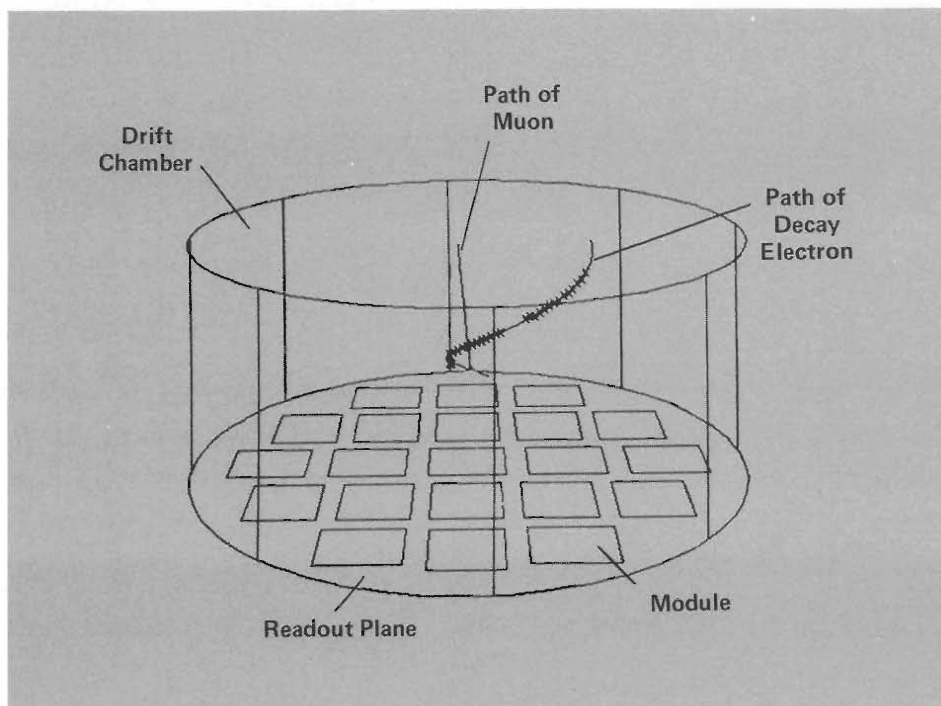


Fig. 12. An example of the typical helical track observed for a muon-decay event in an early run with the TPC. (The detector here is shown on end compared to Fig. 11.)

Gary H. Sanders learned his physics on the east coast, starting at Stuyvesant High School in New York City, then Columbia and an A.B. in physics in 1967, and finally a Ph.D. from the Massachusetts Institute of Technology in 1971. The work for his doctoral thesis, which dealt with the photoproduction of neutral rho mesons on complex nuclei, was performed at DESY's electron synchrotron in Hamburg, West Germany under the guidance of Sam Ting. After seven years at Princeton University, during which time he used the beams at Brookhaven National Laboratory and Fermi National Accelerator Laboratory, he came west to join the Laboratory's Medium Energy Physics Division and use the beams at LAMPF. A great deal of his research has dealt with the study of muons and with the design of the beams, detectors, and signal processing equipment needed for these experiments.



The various scientific teams associated with each experiment are listed below.

Tritium beta decay

Los Alamos National Laboratory:

Thomas J. Bowles, R. G. Hamish Robertson, Martin P. Maley, John F. Wilkerson, John C. Browne, Tom H. Burritt, James S. Cohen, Richard L. Martin, Robert K. Sander, Evan O. Ballard

Princeton University:

David A. Knapp (graduate student)

University of California, San Diego:

Jerry Helfrich (graduate student)

Rare decays of the muon (the Crystal Box)

Los Alamos National Laboratory:

Richard D. Bolton, James D. Bowman, Roger D. Carlini, Martin D. Cooper, M. Duong-van, James S. Frank, Askel L. Hallin, Peter A. Heusi, Cyrus M. Hoffman, Fesseha G. Mariam, H. S. Matis, Richard E. Mischke, Darragh E. Nagle, Vernon D. Sandberg, Gary H. Sanders, Urs Sennhauser, R. L. Talaga, Richard D. Werbeck, Robert A. Williams

Stanford University:

Steven L. Wilson, E. Barry Hughes, Robert Hofstadter

University of Chicago:

David Grosnick, S. Courtenay Wright

Temple University:

Gary E. Hogan, Virgil L. Highland

Neutrino-electron scattering

University of California, Irvine:

Richard C. Allen, Vinod Bharadwaj, George Brooks, Herbert H. Chen, Peter J. Doe, René Hausammann, Wen-Piao Lee, Hans-Jorg Mahler, Minick Rushton, Ken-Chung Wang

Los Alamos National Laboratory:

Thomas J. Bowles, Robert L. Burman, Roger D. Carlini, Donald R. S. Cochran, James S. Frank, Eliezar Piasetzky, Vernon D. Sandberg

University of Maryland:

Danial A. Krakauer, Richard C. Talaga

Prototype for a larger fine-grained neutrino detector

Los Alamos National Laboratory:

Thomas Bowles, Ronald Brown, Robert Burman, Roger Carlini, David Clark, Scott Clearwater, Donald Cochran, Thomas Dombeck, Herald Kruse, David Lee, Vernon Sandberg

University of New Mexico:

Berndt Bassalleck, Byron Dieterle, Roger Hill, Ju Kang, Chris Leavitt

Temple University:

Leonard Auerbach, Suno Datta, Virgil Highland, David Huang, Kenneth McFarlane

University of California, Los Angeles:

Bjarni Aas, George Igo, Charles Newsom

University of California, Riverside:

David Beavis, Sunayana Y. Fung, Bill Gorn, Robert Poe, Gordon Van Dalen

Valparaiso University:

Donald Koetke, Randolph Fisk

University of Texas:

David Oakley

Electron-antineutrino appearance mode experiment

Argonne National Laboratory:

Stuart Freedman, Gerry Garvey, Mike Green, Kevin Lesko, James Napolitano

California Institute of Technology:

Brian Fujikawa, Bob McKeown

Los Alamos National Laboratory:

Roger Carlini, Joey Donahue, Vern Sandberg

Louisiana State University:

Catherine Choi, Ali Fazely, Richard Imlay, Serge Lusin, Bill Metcalf

Ohio State University:

Ron Harper, T. Y. Ling, Joe Mitchell, Thomas Romanowski, Elton Smith, Mark Timko

Normal muon decay (time projection chamber)

Los Alamos National Laboratory:

Herbert L. Anderson, W. Wayne Kinnison, John W. Lillberg, Robert J. McKee

University of Chicago:

Ming-Jen Yang

Swiss Institute for Nuclear Research, Switzerland:

Alex Zehnder

National Research Council, Canada:

Clifford K. Hargrove